

Journal of the WASHINGTON ACADEMY OF SCIENCES



Editor's Comments <i>K. Baclawski</i>	ii
Board of Discipline Editors	iii
Membership Application	iv
Instruction to Authors	v
Affiliated Institutions	vi
The Search for Extrasolar Moons <i>A. Paris</i>	1
Dealing with Disasters <i>K. Baclawski et al.</i>	17
Peak Wavelength Inflection Law <i>T. Kakovitch et al.</i>	49
The Shape of Planck's Law <i>K. Baclawski</i>	57
Affiliated Societies and Delegates	64

Washington Academy of Sciences

Founded in 1898

BOARD OF MANAGERS

Elected Officers

President

Lynnette Madsen

President Elect

Mahesh Mani

Treasurer

David Torain

Secretary

Mala Ramaiah

Vice President, Administration

Terry Longstreth

Vice President, Membership

Mahesh Mani

Vice President, Junior Academy

Paul Arveson

Vice President, Affiliated Societies

Parisa Meisami

Members at Large

Mei Sun

Anne Kornahrens

Judy Staveley

Mina Izadjooy

Past President

Ram D. Sriram

AFFILIATED SOCIETY DELEGATES

Shown on back cover

Editor of the Journal

Kenneth Baclawski

Journal of the Washington Academy of Sciences (ISSN 0043-0439)

Published by the Washington Academy of Sciences

email: editor@washacadsci.org

website: www.washacadsci.org

The Journal of the Washington Academy of Sciences

The *Journal* is the official organ of the Academy. It publishes articles on science policy, the history of science, critical reviews, original science research, proceedings of scholarly meetings of its Affiliated Societies, and other items of interest to its members. It is published quarterly. The last issue of the year contains a directory of the current membership of the Academy.

Subscription Rates

Members, fellows, and life members in good standing receive the *Journal* free of charge. Subscriptions are available on a calendar year basis, payable in advance. Payment must be made in US currency at the following rates.

US and Canada	\$30.00
---------------	---------

Other Countries	\$35.00
-----------------	---------

Single Copies (when available)	\$15.00
--------------------------------	---------

Claims for Missing Issues

Claims must be received within 65 days of mailing. Claims will not be allowed if non-delivery was the result of failure to notify the Academy of a change of address.

Notification of Change of Address

Address changes should be sent promptly to the Academy Office. Notification should contain both old and new addresses and zip codes.

Postmaster:

Send address changes to WAS, Rm 455,
1200 New York Ave. NW
Washington, DC 20005

Academy Office
Washington Academy of Sciences
Room 455
1200 New York Ave. NW
Washington, DC 20005
Phone: (202) 326-8975

MCZ LIBRARY

MAR 20 2023

HARVARD UNIVERSITY

Volume 108
Number 3
Fall 2022

Journal of the

WASHINGTON

ACADEMY OF SCIENCES



Editor's Comments <i>K. Baclawski</i>	ii
Board of Discipline Editors.....	iii
Membership Application	iv
Instruction to Authors	v
Affiliated Institutions	vi
The Search for Extrasolar Moons <i>A. Paris</i>	1
Dealing with Disasters <i>K. Baclawski et al</i>	17
Peak Wavelength Inflection Law <i>T.S. Kakovitch et al</i>	49
The Shape of Planck's Law <i>K. Baclawski</i>	57
Affiliated Societies and Delegates	64

ISSN 0043-0439

Issued Quarterly at Washington DC

EDITOR'S COMMENTS

This issue begins with a study by Antonio Paris of the problem of detecting moons of planets outside of our solar system. Detecting exoplanets is already a formidable task, and it is even more difficult to detect moons of exoplanets. The article proposes a promising new approach using light curves recorded by the Kepler spacecraft.

Disasters, such as the COVID-19 pandemic and Climate Change, have become a frequent topic of public discourse today and have resulted in very large amounts of information generated by government agencies, scientific researchers and industry. The second article presents a study, based on a year-long series of sessions, of the different types of disasters and the information needed to respond to them. It was found that there are many cross-domain linkages between the information resources needed for different kinds of disasters, which offers opportunities for the reuse of information resources and tools for rapidly responding to future disasters.

At the end of the 19th century, physicists were unable to explain the spectrum of electromagnetic radiation emitted by bodies, such as the Sun, using existing theories. The solution to this problem by Max Planck led directly to modern Quantum Theory. Indeed, Planck's constant, which is a fundamental physical constant of foundational importance to Quantum Mechanics, was first introduced in Planck's Law. The last two articles study some aspects of Planck's Law. The first article by Kakovitch, Vane and Lambert propose some new physical interpretations of the second derivative of Planck's Law. In the second article I discuss Planck's Law from an elementary mathematical point of view.

Please send your comments on papers, suggestions for articles, and ideas for what you would like to see in the Journal to editor@washacadsci.org.

Kenneth Baclawski



Journal of the Washington Academy of Sciences

Editor Kenneth Baclawski editor@washacadsci.org

Board of Discipline Editors

The *Journal of the Washington Academy of Sciences* has a eleven member Board of Discipline Editors representing many scientific and technical fields. The members of the Board of Discipline Editors are affiliated with a variety of scientific institutions in the Washington area and beyond — government agencies such as the National Institute of Standards and Technology (NIST); universities such as Georgetown; and professional associations such as the Institute of Electrical and Electronics Engineers (IEEE).

Anthropology	Emanuela Appetiti	eappetiti@hotmail.com
Astronomy	Sethanne Howard	sethanneh@msn.com
Behavioral and Social Sciences	Carlos Sluzki	csluzki@gmu.edu
Biology	Poorva Dharkar	poorvadharkar@gmail.com
Chemistry	Deana Jaber	djaber@marymount.edu
Environmental Natural Sciences	Terrell Erickson	terrell.erickson1@wdc.nsda.gov
Health	Robin Stombler	rstombler@auburnstrat.com
History of Medicine	Alain Touwaide	atouwaide@hotmail.com
Operations Research	Michael Katehakis	mnk@rci.rutgers.edu
Science Education	Jim Egenrieder	jim@deepwater.org
Systems Science	Elizabeth Corona	elizabethcorona@gmail.com



Washington Academy of Sciences
1200 New York Avenue
Rm 455
Washington, DC 20005

Please fill in the blanks and send your application to the address above. We will contact you as soon as your application has been reviewed by the Membership Committee. Thank you for your interest in the Washington Academy of Sciences.

(Dr. Mrs. Mr. Ms)

Business Address

Home Address

Email

Phone

Cell Phone

preferred mailing address

Type of membership

Business Home

Regular

Student

Schools of Higher Education attended	Degrees	Dates

Present Occupation or Professional Position

Please list memberships in scientific societies – include office held

Instructions to Authors

1. Deadlines for quarterly submissions are:

Spring – February 1
Summer – May 1

Fall – August 1
Winter – November 1

2. Draft Manuscripts using a word processing program (such as MSWord), not PDF. We do not accept PDF manuscripts.
3. Papers should be 6,000 words or fewer. If there are seven or more graphics, reduce the number of words by 500 for each graphic.
4. Include an abstract of 150-200 words.
5. Use Times New Roman, font size 12.
6. Include two to three sentence bios of the authors.
7. Graphics must be easily resizable by the editor to fit the Journal's page size. Reference the graphic in the text.
8. Use endnotes or footnotes. The bibliography may be in a style considered standard for the discipline or professional field represented by the paper.
9. Submit papers as email attachments to the editor at editor@washacadsci.org.
10. Include the author's name, affiliation, and contact information – including postal address. Membership in an Academy-affiliated society may also be noted. It is not required.
11. Manuscripts are peer reviewed and become the property of the Washington Academy of Sciences.
12. There are no page charges.

Washington Academy of Sciences Affiliated Institutions

National Institute for Standards & Technology (NIST)
Meadowlark Botanical Gardens
The John W. Kluge Center of the Library of Congress
Potomac Overlook Regional Park
Koshland Science Museum
American Registry of Pathology
Living Oceans Foundation
National Rural Electric Cooperative Association (NRECA)

The Search for Extrasolar Moons: Photon Flux Perturbations of Kepler Transit Light Curves

Antonio Paris

Planetary Sciences, Inc.

Abstract

In this study, we expand the discussion of extrasolar planetary research by proposing a new approach to detecting extrasolar moons using Kepler (K2) light curves. We shaped this investigation by comparing transit light-curve data of 5×10^3 main-sequence stars cataloged in NASA's Exoplanet Archive, Radio Galaxy Zoo's Exoplanet Explorers and the Exoplanet Follow-up Observing Program (ExoFOP), which served as the repository to collect and analyze supplementary K2 data. By examining K2 light curves, various characteristics related to transits were modeled, which we then compared with confirmed extrasolar planets, variable stars such as eclipsing binaries and noise or gaps in the data. For illustration, perturbations in the timing of two separate transits for 2MASS J08251369+1425306 ($R_S \approx 0.346\odot$) produced two characteristic decreases in the photon flux (ΔF) followed by two increases, inferring the presence of an extrasolar planet ($R_P \approx 0.0129\oplus$) and its companion, an extrasolar moon ($R_M \approx 0.0048\oplus$). To test our hypothesis, we scrutinized various competing assumptions to resolve the source of the duo-photon flux, namely the *Rossiter-McLaughlin* effect, limb darkening, a multiplanet system or a planet occulting one or more sunspots on the surface of the star. However, we uncovered no analogous light curve in K2 to fit the competing hypotheses and account for the proposed extrasolar planet's companion.

Introduction

LAUNCHED IN 2009, THE KEPLER SPACECRAFT was designed to survey our region of the Milky Way galaxy to discover Earth-size extrasolar planets in or near the habitable zone and to explore the structure and diversity of extrasolar planetary systems.¹ Kepler, which was launched into an Earth-trailing orbit, monitored the brightness of approximately 530,506 stars in a fixed field of view.² Specifically, the spacecraft observed a 100 sq. degree patch of the sky near Cygnus, Lyra and Draco; and rotated by 90 degrees every 90 days to keep the solar panels pointing at the sun.³ This is also the direction of the Solar System's motion around the center of the galaxy. Thus, the stars that Kepler observed are roughly the same distance from the galactic center as the Solar System, and close to the

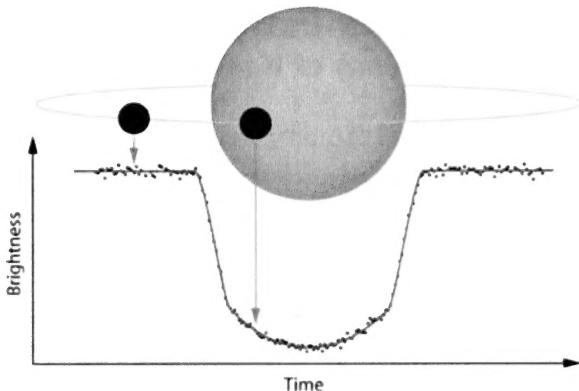


Figure 1: A simulation of a transit light curve as the extrasolar planet blocks light from its parent star. (Source: NASA)

galactic plane. This fact is important if the position in the galaxy is related to habitability, as suggested by the Rare Earth hypothesis. Kepler's data, moreover, are divided into 90-day quarters.⁴ These data were transmitted to Earth, then analyzed to detect periodic dimming (light curves) caused by extrasolar planets when they cross (transit) in front of their parent star. On October 30, 2018, the Kepler spacecraft's end of mission was declared, with the spacecraft finally running out of fuel.⁵ During its nine years in orbit, Kepler observed a total of 150,000 main-sequence stars and discovered 2,662 planets, many of which could be promising places for life.⁶

The Transit Method for Detecting Extrasolar Planets

Through the use of photometry, the Kepler spacecraft used the transit method to detect extrasolar planetary systems. This technique consists of regularly observing a star to detect the periodic decrease in luminosity (ΔF), also known as flux, associated with the transit of an extrasolar planet.⁷ Both the size of the parent star and the extrasolar planet will determine ΔF during the transit. For illustration, for a star the size of the Sun, the transit of a Jupiter-sized planet will cause a decrease in the apparent luminosity of $\approx 1\%$, whereas this decrease will be $\approx 0.001\%$ for a planet the size of the Earth.⁸ When extrasolar planets pass in front of their host star (as seen from Earth), moreover, a decrease in the photon flux can be measured over time to allow for the construction of a light curve (Figure 1). By measuring ΔF and knowing the size of the parent star, we

can determine the size or radius of the extrasolar planet, its orbital period and, using Kepler's Third Law of Planetary Motion, the average distance of the extrasolar planet from its parent star can be determined.⁹

Data Collection

Kepler Spacecraft: Kepler's primary high reflectance mirror is 1.4 meters (4.6 ft) in diameter with a 100 deg² (\approx 12-degree diameter) field of view. The spacecraft's telescope has a Schmidt camera with a 0.95 meter (37.4 in) front corrector plate (lens) feeding a 1.4 meter (55 in) primary mirror. The mirror was specifically designed with sufficient sensitivity to detect relatively small extrasolar planets as they transit their parent star.¹⁰ At the time, the mission objective was a combined differential photometric precision of 20 parts per million on a magnitude 12 star for a 6.5 hour integration.¹¹ The photometer, moreover, has a soft focus to provide photometry, rather than sharp images. The focal plane of the spacecraft's camera, furthermore, is made from 42 50 mm \times 25 mm (2 in \times 1 in) CCDs at 2200 \times 1024 pixels each, possessing a total resolution of 94.6 megapixels.¹² The data from these pixels were then requantized, compressed and stored in the onboard 16 gigabyte solid-state recorder.

Kepler 2 (K2) Data Sets: There are two archives for official Kepler and K2 data products—the Exoplanet Archive, which is hosted at the NASA Exoplanet Science Institute and the Mikulski Archive for Space Telescopes (MAST), which is hosted at the Space Telescope Science Institute (STScI). The Exoplanet Archive primarily hosts data related to the Kepler and K2 mission exoplanet searches.¹³ MAST, on the other hand, is responsible for hosting time series data and spacecraft calibration products for Kepler and K2.¹⁴ In addition, this research has made use of the Exoplanet Follow-up Observation Program (ExoFOP), which is operated by the California Institute of Technology, under contract with NASA under the Exoplanet Exploration Program. For this investigation, ExoFOP served as the repository to collect and analyze community-gathered data related to K2, including the light curves presented hereafter.

2MASS: The summary of stellar information used in this investigation was obtained using data products from the Two Micron All Sky Survey (2MASS), which is a joint project of the University of Massachusetts and the Infrared Processing and Analysis Center/California Institute of Technology, funded by NASA. The data were collected by 1.3 m telescopes at

Mt. Hopkins and CTIO, Chile, which, thereafter, created the Point Source Catalog consisting of over 500 million stars and galaxies, the Extended Source Catalog consisting of 1.6 million resolved galaxies and the Large Galaxy Atlas consisting of ≈ 600 nearby galaxies and globular clusters.¹⁵ The stellar information throughout this study includes galactic coordinates, star magnitude and classification, and distance in parsecs.

Radio Galaxy Zoo: Additional light-curve data for this investigation were obtained from Exoplanet Explorers. The archival data are part of Radio Galaxy Zoo—an Internet-crowdsourced citizen science project. Through the use of K2 data, citizen scientists assisted scientists in identifying potential transiting extrasolar planets. The program is hosted by the web portal Zooniverse. To date, data from Kepler's survey revealed over 4,000 candidate extrasolar planets—many of which were identified by citizen scientists participating in the Exoplanet Explorers project.¹⁶

Comparing Kepler Transit Light Curves

Numerous astrophysical processes can impersonate planetary transits. Light-curve data sets cataloged in K2 primarily consist of confirmed and/or candidate extrasolar planets, variable stars such as eclipsing binaries and pulsating stars, and noisy data with light curves that have such scattered data points that it is difficult to determine if a valid signal was collected by Kepler. By comparing these light curves, it is then possible to compare the processes at work within each stellar object and/or event.¹⁷ When we plot a new light curve obtained by Kepler, we can compare it to those standard light curves previously observed by other astronomical surveys. Through these methods, therefore, we can attempt to identify the type of object observed by Kepler. For illustration, the light curve for the confirmed extrasolar planet K2-14 b (Figure 2) produced a *flat* light curve with one clear “U-shaped” dip centered at time 0.0.¹⁸ Moreover, when K2-14 b passed behind its parent star at time ≈ 0.13 , the light from the extrasolar planet, such as starlight that was reflecting off the planet's surface, was blocked by the parent star. This decrease in brightness is known as a “secondary eclipse.”¹⁹

Although multiplanet light curves produce comparable “U-shaped” dips in their folded light curve, these systems can be differentiated from single-planet systems by *unfolding* their individual transits. The main-sequence star K2-14, for example, is known to host only one confirmed

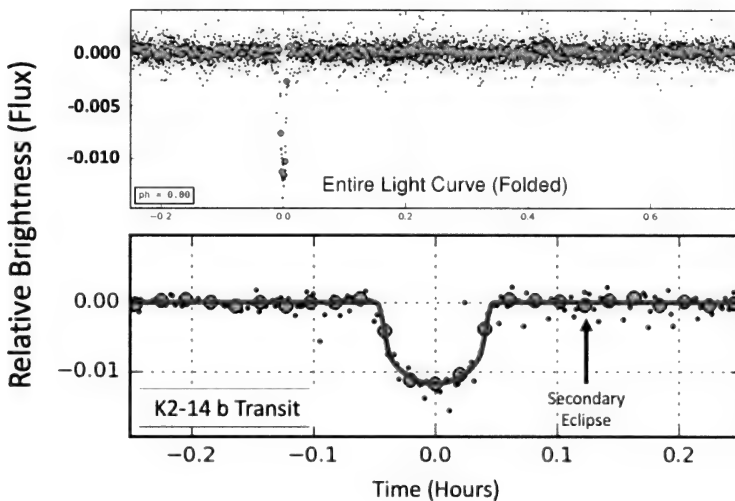


Figure 2: Light curve for K2-14 b (Source: Exoplanet Explorers and ExoFOP)

planet (K2-14 b). When we unfold the light curve for K2-14 b, the data reveal nine separate transits with comparable U-shaped dips at ≈ 0.0 .²⁰ In contrast, the unfolded light curve for a multiplanet system, such as K2-138 (six known planets), produced transits with dissimilar light curves (Figure 3).²¹

Some transits are caused by other stars rather than a planet. One type of variable star, such as an eclipsing binary, varies dramatically in brightness in a regular cycle. Eclipsing binaries are a pair of stars that orbit each other—one star will transit in front and behind the other, as seen by Kepler. Their light curves, consequently, will generate *deep dips* and the entire folded light curve will produce a sinusoidal pattern as opposed to a flat light curve. To demonstrate, the light curve for the confirmed eclipsing binary star 2MASS J12232783-0649416 (Figure 4) has a deep minimum when eclipsed at time ≈ 0.0 and a shallower minimum when the dimmer star is eclipsed at ≈ 0.5 (folded light curve).²² Furthermore, the folded light curve is sinusoidal as opposed to flat.

Some stars, such as pulsating variable stars, vary dramatically in brightness in their regular cycle. The radius of this type of star alternately expands and contracts as part of its natural evolutionary aging processes.²³ Their light curves, therefore, are distinctive and show a rapid

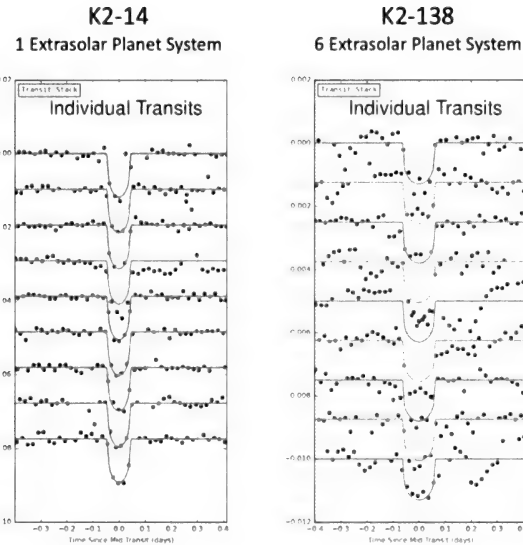


Figure 3: Comparing individual transits for K2-14 and K2-138
 (Source: Exoplanet Explorers and ExoFOP)

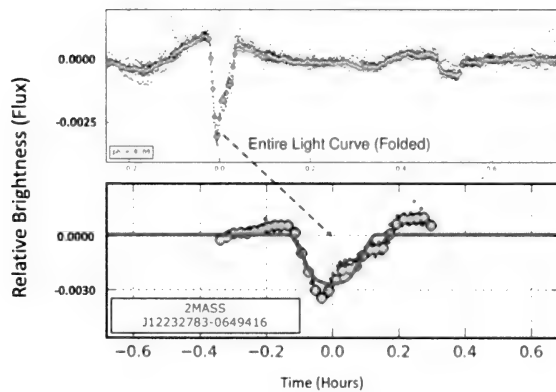


Figure 4: Light curve for 2MASS J12232783-0649416
 (Source: Exoplanet Explorers and ExoFOP)

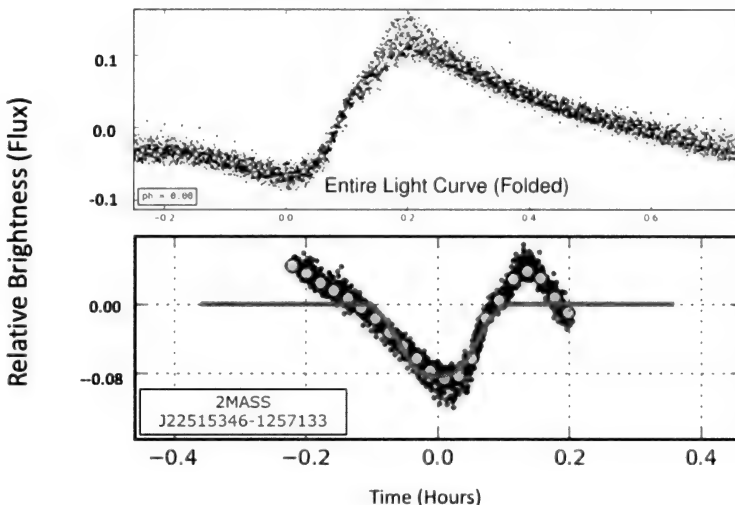


Figure 5: Light curve for 2MASS J22515346-1257133
 (Source: Exoplanet Explorers and ExoFOP)

rise in brightness followed by a smoother decline, shaped like a shark fin.²⁴ The light curve for the star 2MASS J22515346-1257133 (Figure 5), for instance, shows the characteristic rapid rise at time ≈ 0.2 in brightness when the star expands followed by a more gradual decrease as the star's radius contracts.²⁵

Some light curves have scattered (noisy) data or missing data points so that it is difficult to determine if a valid signal and/or observation was collected by Kepler. The principal source of noise in K2 data was created by the motion of the Kepler spacecraft due to periodic thruster firings. This caused stars to drift across different pixels on the detector, which have varied sensitivity.²⁶ The light curve for the star 2MASS J03355065+1654303 (Figure 6) visibly displays noise and missing data, and as such, is not an acceptable candidate for extrasolar planet surveys.²⁷

Proposed Methodology for Identifying Extrasolar Moons

Extrasolar moons are detectable for the same reasons their parent planets are—they have mass and occupy space.²⁸ By analyzing K2 perturbations in the timing of transits, it is possible to infer the presence of additional planetary companions, including extrasolar moons.²⁹ However,

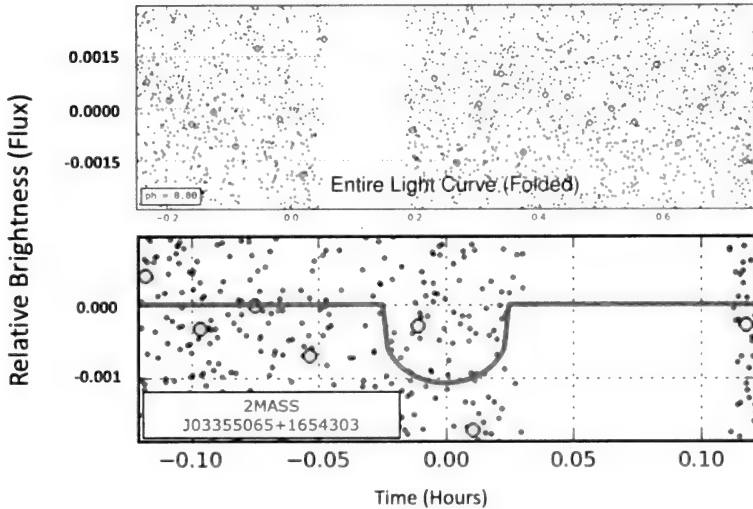


Figure 6: Light curve for 2MASS J03355065+1654303
 (Source: Exoplanet Explorers and ExoFOP)

before searching for extrasolar moons using K2 data, we first have to consider an essential question: would it be possible to detect an extrasolar moon around a main-sequence star, given the current quality of K2 data? As we demonstrate in our simulation below (Figure 7), we posit, when an extrasolar moon begins to block the light from the parent star (Event A) the initial transit should produce a slight dip in the light curve (D_A). Afterward, when the extrasolar planet blocks the starlight during its transit (Event B), it should then produce the typical U-shaped light curve (D_B). Similarly, when the extrasolar moon begins to egress from the transit (Event C), an increase in luminosity from the parent star will produce a slight increase in the light curve (I_C) followed by a substantial increase (I_D) as the extrasolar planet exits the transit (Event D).

Assuming the star's radius (R_S) is known, the light curve will also provide an estimate for the radius of the extrasolar planet (R_P) and its moon (R_M) by determining the fraction of starlight, ΔF , that was blocked. Although the equation assumes the stellar disc has a uniform brightness, as a preliminary estimate the mathematical relationship (Equations 1 and 2) works quite well.³⁰

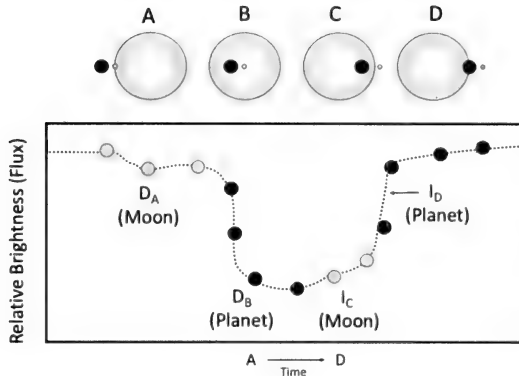


Figure 7: A simulation of transit light curve for an extrasolar planet with a companion moon. (Source: Planetary Sciences, Inc.)

$$\text{Radius of Planet} \quad \Delta F = R_P^2 / R_S^2 \quad \text{whereas} \quad R_P = R_S \sqrt{\Delta F} \quad (1)$$

$$\text{Radius of Exomoon} \quad \Delta F = R_M^2 / R_S^2 \quad \text{whereas} \quad R_M = R_S \sqrt{\Delta F} \quad (2)$$

Data Analysis and Interpretation

A random sampling of 5×10^3 K2 light curves archived in the Exoplanet Explorers project, then cross-referenced with ExoFOP, revealed eight light curves (Table 1) analogous to the extrasolar moon-like perturbations described in our simulation (Figure 7).

EE Subject ID	EPIC ID (ExoFOP)	2MASS ID	Ra (deg)	Dec (deg)	Distance (pc)	Radius (R_{Sun})	Mass (M_{Sun})
7775826	211591558	J08251369+1425306	126.307076	14.42519	312.9	0.346	0.356
7608624	201456770	J12224737-0007187	185.697449	-0.121909	5.82E+02	0.926	0.891
7654197	210924845	J04042735+2147014	61.113998	21.78367	108.4	1.549	1.192
7774537	211430475	J08512348+1206040	132.847855	12.101128	5.62E+02	0.308	0.329
7775208	211527627	J08142873+1331468	23.619728	13.529658	179.3	0.446	0.503
7775402	211545599	J08170774+1346494	124.282227	13.780388	2289	28.395	1.124
7605568	201192009	J12081933-0417229	182.080521	-4.289704	3.16E+03	4.955	0.893
7775832	211592036	J08253940+1425538	126.414192	14.431643	641	1.456	1.168

Table 1: List of eight light curves exhibiting extrasolar moon-like perturbations. (Source: Exoplanet Explorers (EE Subject ID) and ExoFOP (EPIC ID)).

Consider the light curve for 2MASS J08251369+1425306 (K2 Campaign: 5), a main-sequence star located $\approx 319\text{pc}$ from Earth (Figure 8).³¹

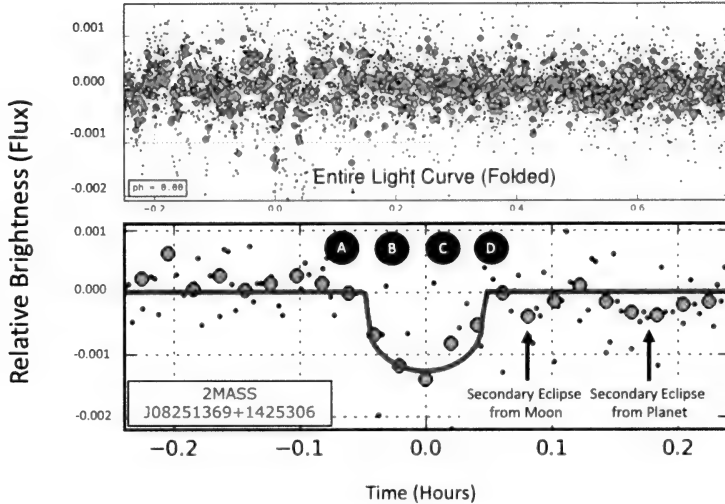


Figure 8: Light curve data for 2MASS J08251369+1425306 with corresponding events A-D. (Source: Exoplanet Explorers and ExoFOP)

As the proposed extrasolar moon began to block the light from the star (Event A) at time -0.1 the transit generated a minor dip ($\Delta F \approx 0.0002$) in the light curve. Subsequently, when the proposed extrasolar planet blocked the starlight during its transit (Event B), it then produced the corresponding U-shaped light curve at phase 0.0 ($\Delta F \approx 0.0014$). Afterward, when the proposed extrasolar moon exited its transit of the parent star (Event C), the increase in luminosity generated a minor increase in the light curve, followed by an increase in the flux when the extrasolar planet exited the transit (Event D).

With reference to Equation 1, because the radius for 2MASS J08251369+1425306 is known (Table 1), we can estimate the radius of the extrasolar planet (Equations 3 and 4) using the fraction of starlight, $\Delta F \approx 0.0014$, that was blocked (Figure 8) at transit times -0.06 to 0.0.

$$R_P = R_S \sqrt{\Delta F} \quad \text{whereas} \quad R_P = 0.346 \sqrt{0.0014} \quad (3)$$

$$R_P \approx 0.0129 \quad (4)$$

Correspondingly, we can also estimate the radius of the extrasolar moon (Equations 5 and 6) using the fraction of starlight, $\Delta F \approx 0.0002$, that was

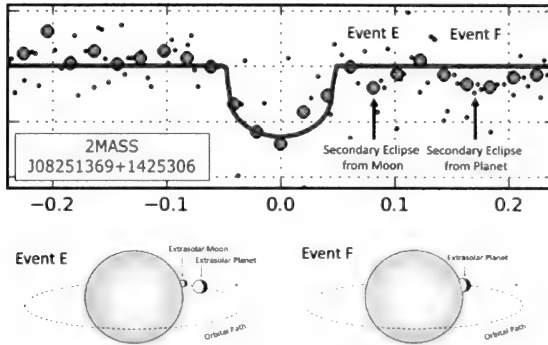


Figure 9: Post-transit light curve for first secondary eclipse (Event E) and second secondary eclipse (Event F).

(Source: EE Explorers and Planetary Sciences, Inc.)

blocked (Figure 8) at transit times -0.1 to -0.06.

$$R_M = R_S \sqrt{\Delta F} \quad \text{whereas} \quad R_M = 0.346 \sqrt{0.0002} \quad (5)$$

$$R_M \approx 0.0048 \quad (6)$$

The folded light curve, furthermore, exhibits a pair of secondary eclipses that we infer are associated with when the extrasolar moon and planet were occulted by 2MASS J08251369+1425306. The first and shorter secondary eclipse at time ≈ 0.08 (Event E) is the light from the extrasolar moon's dayside being blocked as it makes its orbit *behind* the star (Figure 9). Similarly, a subsequent and lengthier secondary eclipse was generated at time ≈ 0.17 (Event F) when the extrasolar planet (which is larger) made its orbit *behind* the star.

Competing Hypotheses for the Source of the Photon Flux Perturbations

Numerous astrophysical processes occur during planetary transits that can account for the source of the duo-photon flux (double dip) associated with 2MASS J08251369+1425306. The Rossiter-McLaughlin effect, for illustration, is a natural phenomenon that occurs during a planetary transit and can generate dips in the light curve resembling the perturbation from the proposed extrasolar moon. The anomaly occurs in part due

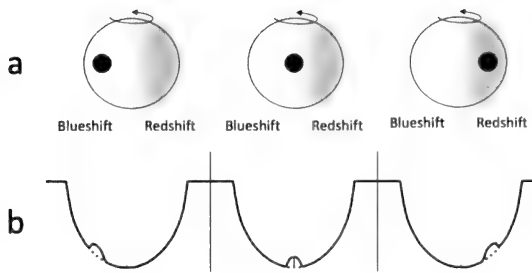


Figure 10: Simulation of Rossiter-McLaughlin effect (a) and associated light curves (b). (Source: Planetary Sciences, Inc.)

to the doppler reflex motion that an orbiting planet imparts on its rotating parent star (Figure 10a). As the parent star rotates on its axis, one side of its photosphere will be seen to be coming toward the viewer (blueshifted) while the other visible quadrant appears to be moving away (redshifted). When the extrasolar planet transits the parent star, it blocks part of the latter's disc, preventing some of the blue- and redshifted light from reaching the observer. As a result, the transit will appear as an anomalous radial-velocity variation on the light curve (Figure 10b).³² Although some studies have speculated on the prospects of using K2 data to detect extrasolar planets using the Rossiter-McLaughlin effect, it will be difficult to detect transits using this method due to the limitations of Kepler's instruments.³³ Therefore, we ruled out the Rossiter-McLaughlin effect as the source of the perturbations.

Photons escaping the edge of the stellar disc, where the temperature is cooler due to altitude and the radiation is less intense, will cause the star to appear darker along its outer edges (Figure 11a).³⁴ This phenomenon, known as *limb darkening*, causes the photons emitted from the limb of the stellar disc to follow a more oblique path through the stellar atmosphere than the photons emitted from the center.³⁵ Limb darkening, however, depends on the spectrum (i.e., visible vs infrared) being used to observe the star.³⁶ The limb-darkening effect is largest at short wavelengths where a highly rounded light curve is observed. Conversely, as the effective stellar temperature increases, the transit light curve becomes shallower and wider (Figure 11b). However, for the purposes of this investigation, the effects of limb darkening have already been modeled into K2 light curves with limb

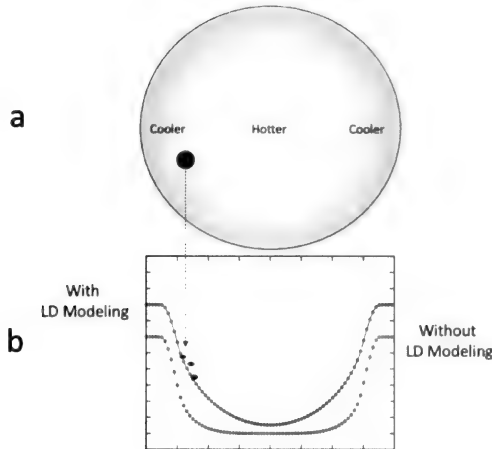


Figure 11: Simulation of limb-darkening effect on light curves.
(Source: Planetary Sciences, Inc.)

darkening coefficients.

Our final hypothesis to account for the perturbations is sunspots—dark blotches on the surface of the star associated with intense magnetic activity. The temperatures of these sunspots are lower than the rest of the photosphere, which gives them their dark appearance.³⁷ As the star rotates, sunspots will come in and out of view causing changes in the star's brightness. The pattern in the star's light curve, therefore, will repeat once per rotation period of the star. As a result, the sunspot will produce a small bump in the transit light curve until the sunspot's lifecycle ends (Figure 12). However, because the light curve for 2MASS J08251369+1425306 was assembled from five separate transits, the sunspot should have formed multiple perturbations along the light curve—which was not evident in the K2 data we analyzed.

Conclusions

Our investigation of K2 light curves established that extrasolar moons are detectable by inspecting the perturbations in the timing of transits produced by multiple celestial bodies orbiting their parent star. Of the 5×10^3 main-sequence stars we examined, at least eight of the stars revealed light curves analogous to the extrasolar moon-like perturbations demon-

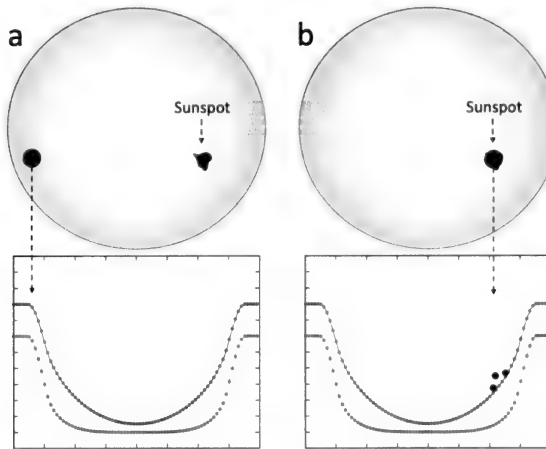


Figure 12: A simulation of an extrasolar planet occulting a sunspot.
 (Source: Planetary Sciences, Inc.)

strated in our simulation. The two individual decreases in the photon flux associated with 2MASS J08251369+1425306, we postulate, imply the presence of an extrasolar planet with a radius of $R_P \approx 0.129$ and its companion, an extrasolar moon, with a radius of $R_M \approx 0.0048$. During our investigation, moreover, we analyzed four other astronomical anomalies that could account for the perturbations, namely the Rossiter-McLaughlin effect, limb darkening, a multiplanet system or the occultation of a sunspot on the surface of the star. A review of the main-sequence stars we examined, however, found no analogous K2 light curves to accommodate our competing hypotheses and/or account for the perturbations associated with 2MASS J08251369+1425306.

References

1. NASA. (2018). Kepler and K2. Mission Overview. <https://bit.ly/3Z6PB8q>
2. NASA. (2020). NASA's Kepler Mission by the Numbers. <https://bit.ly/3Qh43GQ>
3. NASA. (2009). Kepler: NASA's First Mission Capable of Finding Earth-Size Planets (PDF). <https://bit.ly/3GJ9JX5>
4. Mikulski Archive for Space Telescopes. (2009). Kepler Mission and Data Fact Sheet. <https://bit.ly/3GhC1qh>
5. Davenport, Justin. (2018). Kepler – NASA's Planet-Hunting Spacecraft – Retired after Running out of Fuel. Spaceflight Now. <https://bit.ly/3GhKWI9>

6. NASA. (2018). Kepler and K2. NASA Retires Kepler Space Telescope, Passes Planet-Hunting Torch. <https://bit.ly/3VQ9sWP>
7. Institute for Research on Exoplanets. (n.d.). Transit Method. <https://bit.ly/3X7MAmv>
8. Astronomy Wiki. (n.d.) Transit Method. <http://bit.ly/3GGte2C>
9. NASA. (2021). Light Curve of a Planet Transiting Its Star. <https://bit.ly/3GJ9YRZ>
10. Fulton L., Michael; Dummer, Richard S. (2011). Advanced Large Area Deposition Technology for Astronomical and Space Applications. Vacuum & Coating Technology (December 2011): 43–47. <https://bit.ly/3WQQujX>
11. Gilliland, Ronald L.; et al. (2011). Kepler Mission Stellar and Instrument Noise Properties. The Astrophysical Journal Supplement Series. 197. <https://bit.ly/3WP0DxH>
12. Caldwell, Douglas A., et al. (July 2010). Kepler Instrument Performance: An In-Flight Update. Proceedings of SPIE. Space Telescopes and Instrumentation 2010. <https://bit.ly/3WOrpWX>
13. California Institute of Technology. (n.d.). NASA Exoplanet Archive. <https://bit.ly/3jUkVHw>
14. Mikulski Archive for Space Telescopes. (2018). Kepler Mission and Data Fact Sheet. <https://bit.ly/3ibYKw1>
15. California Institute of Technology. (n.d.). Two Micron All Sky Survey (2MASS). <https://bit.ly/3ZfPWWj>
16. Zoo Universe. (2022). Exoplanet Explorers. <https://bit.ly/3Zcjt3j>
17. NASA. (2013). Light Curves and What They Can Tell Us. <https://bit.ly/3IouVTy>
18. Exoplanet Explorers. (2022). K2 Subject 8492681. <https://bit.ly/3QhxNNo>
19. Vanderburg, Andrew. (n.d.). The Transit Light Curve. <https://bit.ly/3Qi8H7w>
20. Exoplanet Explorers. (2022). K2 Subject 8492681. <https://bit.ly/3Cr8zga>
21. Exoplanet Explorers. (2022). K2 Subject 8496743. <https://bit.ly/3XacOoE>
22. Exoplanet Explorers. (2022). K2 Subject 7615625. <https://bit.ly/3VXngik>
23. Toppr. (n.d.). Stars and the Solar System. Variable Star. <https://bit.ly/3vIfmyu>
24. Australian Telescope National Facility. (n.d.). Pulsating Variable Stars. <https://bit.ly/3vESpw4>
25. Exoplanet Explorers. (2022). K2 Subject 7606298. <https://bit.ly/3WSjGak>
26. NASA. (2020). K2: Extending Kepler's Power to the Ecliptic. <https://bit.ly/3ioDVgG>

27. Exoplanet Explorers. (2022). K2 Subject 7633359. <https://bit.ly/3XbQQBl>
28. Smith, Steven. (2013). Would it be possible to find a moon around an extrasolar planet? If so, how? *Astronomy Magazine*. <https://bit.ly/3CrVMdL>
29. Wilson, Paul. (n.d.). The Exoplanet Transit Method. <https://bit.ly/3jVa5Ry>
30. Futurism. (2013). The Transit Method: Finding Other Worlds. <https://bit.ly/3GL2n5C>
31. EXOFOP. (2022). Target 2MASS J08251369+1425306. <https://bit.ly/3GITbOZ>
32. Ohta, Yasuhiro. (2004). The Rossiter-McLaughlin Effect and Analytic Radial Velocity Curves for Transiting Extrasolar Planetary Systems. *The Astrophysical Journal Supplement Series*. 623. <https://bit.ly/3VN2uBS>
33. Gaudi, B. Scott; (2006). Prospects for the Characterization and Confirmation of Transiting Exoplanets via the Rossiter-McLaughlin Effect. *The Astrophysical Journal Supplement Series*. 655. <https://bit.ly/3GrrHMC>
34. Fischer, Debra A. (2015). *Exoplanet Detection Techniques*. University of Arizona Press, Tucson, 914 pp. <https://bit.ly/3Gkj5aj>
35. European Space Agency. (2022). Exoplanet Detection Methods. <https://bit.ly/3VPT9sI>
36. Sing, David K. (2018). Stellar Limb-Darkening Coefficients for CoRot and Kepler. *Astronomy & Astrophysics*. <https://bit.ly/3GnEKhI>
37. Zoo Universe. (2022). Planet Hunters. Starspots and Transits. <https://bit.ly/3X6W4yy>

ANTONIO PARIS, the Principal Investigator for this study, is the Chief Scientist at Planetary Sciences, Inc., an Assistant Professor of Astronomy and Astrophysics at St. Petersburg College, FL, and a graduate of the NASA Mars Education Program at the Mars Space Flight Center, Arizona State University. He is a professional member of the Washington Academy of Sciences, the American Astronomical Society and The Explorers Club; and his latest peer-reviewed publication focused on broad-line quasars—active galactic nuclei emissions powered by supermassive black holes.

Ontology Summit 2022 Communiqué

Dealing with Disasters

Kenneth Baclawski¹, Michael Bennett², Gary Berg-Cross³
Robert J. Rovetto⁴, Ravi Sharma⁵, Ram D. Sriram⁶

¹Northeastern University, ²Hypercube Limited, London

³ESIP Semantic Harmonization, ⁴Independent consultant, ⁵Senior Enterprise Architect
⁶National Institute of Standards and Technology

Abstract

The COVID-19 pandemic as well as other recent disasters have prompted an impressive, worldwide response by governments, industry, and the academic community. A newfound willingness both to share information and to improve transparency in sharing information has played a role in the success of these responses. In this article we examine the landscape of health-related, environmental, and aerospace disasters; and a framework consisting of a set of dimensions is developed to characterize the landscape. A sample of projects is presented to illustrate best practices and lessons learned for tasks such as search, data description, interoperability and harmonization of the increasingly large data sources that are relevant to disasters. It was found that there are many cross-domain linkages between the information resources needed for responding to different kinds of disasters, which offers opportunities for the reuse of information resources.

1. Introduction

THE UNITED NATIONS OFFICE FOR DISASTER RISK REDUCTION (UNDRR) defines a disaster to be “a serious disruption of the functioning of a community or a society at any scale due to hazardous events interacting with conditions of exposure, vulnerability and capacity, leading to one or more of the following: human, material, economic and environmental losses and impacts” (UNDRR, 2022). The International Federation of Red Cross and Red Crescent Societies (IFRC) adds the requirement that the disruption must exceed the capacity or willingness of a community or society to cope using its own resources (IFRC, 2022). By the IFRC definition, an emergency would not be a disaster if the community or society has the capacity and willingness to cope. While preventing all possible disasters is

not possible, one can reduce disaster risks either by addressing the underlying causes of the emergencies that can result in disasters or by ensuring that there are adequate resources and plans for coping with foreseeable emergencies to prevent them from becoming disasters (by the IFRC definition). Information is fundamental to either way of reducing disaster risks; indeed, one can argue disasters are nearly always the result of a failure of information (West, 2022). When a disaster has occurred, information is necessary for managing the disaster.



Figure 1: Pictorial Representation of the Landscape of Kinds of Disaster (Ravi Sharma)

New technologies, better sensors and greater willingness to share data have increased the quantity and complexity, as well as the timeliness, of information in general, and of information that is relevant for disaster risk reduction and disaster management in particular. As a result of the increase in volume, complexity, and creation speed of data, we increasingly

rely on computational support to deal with data. The Findability, Accessibility, Interoperability, and Reuse (FAIR) principles are guidelines to ensure that data is machine-actionable with minimal or no human intervention (GO FAIR, 2022). The FAIR guidelines require data to be described with rich metadata, and both data and metadata must conform to the FAIR principles. However, to make data FAIR whilst preserving them over time requires trustworthy digital repositories with sustainable governance and organizational frameworks, reliable infrastructure, and comprehensive policies supporting community-agreed practices. The Transparency, Responsibility, User focus, Sustainability and Technology (TRUST) principles were collaboratively developed and endorsed by the digital repository community for the purpose of providing a common framework to facilitate discussion and implementation of best practice in digital preservation by all stakeholders (Lin, D., Crabtree, J., Dillo, I. et al., 2020). Semantic technologies (also called knowledge organization systems) can be useful for coping with the variety of sources and types of information by meaningfully harmonizing data from diverse sources and by aiding interoperability of systems for disaster risk reduction as well as disaster management systems helping to ensure that data and metadata satisfies FAIR and TRUST principles. Semantic technologies can range from simple taxonomies to formal ontologies. An ontology encompasses a representation, formal naming, and definition of the categories, properties, and relations between the concepts, data, and entities that substantiate one, many, or all domains of discourse.

In this article we begin by developing a framework for the dimensions that define disasters. A pictorial representation of the framework is shown in Figure 1. While disasters have many common features and generally follow similar lifecycles, there are differences that influence the kinds of technologies that are best suited to risk reduction and management. This is especially the case for ontologies, and we discuss the issues and make recommendations in Section 2.

The disaster that has generated the most public attention in recent times is the COVID-19 pandemic. The COVID-19 pandemic has had a massive impact on the world, in terms of human toll – economically, socially, politically and scientifically. Section 3 is devoted to pandemics with special attention to COVID-19.

There is a very wide range of environmental disasters. The most

prominent are climate change, wildfires, and floods. Section 4 discusses environmental disasters and the issues that they raise. Aerospace and maritime disasters are considered in Section 5.

In Section 6, we present a representative sample of projects that have developed and use semantic technologies and ontologies for disaster monitoring and management. The projects illustrate the usefulness of semantic technologies such as ontologies for many purposes as well as provide lessons for developers who need to respond to hazards, emergencies and other disruptions.

2. Disaster Framework Dimensions

Disasters can be characterized by a number of dimensions. We organized the dimensions using the basic question words whose answers are considered foundational for information gathering, problem solving, defining an enterprise, or establishing a context (Baclawski et al, 2020b; Bennett, 2021). The questions are shown in Figure 2. In addition, we included some dimensions that are relevant to disasters: risk, severity, and supply chains. Finally, the degree to which any data or metadata conforms to FAIR and TRUST principles is an important dimension.

Whence. The first question is concerned with the origin or cause of a disaster. This is more subtle than it might seem. For example, it seems obvious that since the COVID-19 disease is caused by the SARS-CoV-2 virus, the COVID-19 pandemic was caused by this virus. However, that misrepresents the full lifecycle situation. At its initial stages, a pandemic begins as a local health emergency. The emergency can then progress to a local epidemic, and only when it spreads uncontrollably does it emerge as an epidemic or pandemic. The same is true for disasters in general; a risky situation may emerge as an emergency, becoming a disaster only when it can no longer be managed using available resources and plans. The inadequacy of available resources and the subsequent need for outside assistance that is more properly a necessary ingredient or cause of a disaster. The lack of available resources, in turn, is generally the result of an information failure due to poor communication, insufficient adequate knowledge, lack of access to relevant information, or other information failures (West. 2022). Accordingly, information is fundamental to understanding the cause of a disaster as well as how best to respond to it. Resources such as ontologies can play an important role in structuring information relevant to a disaster

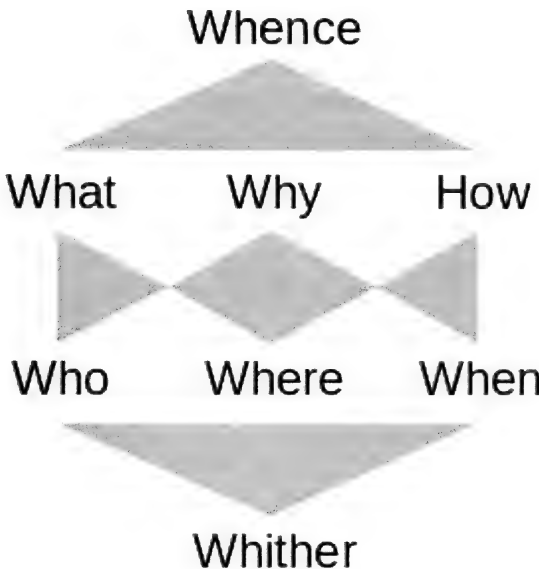


Figure 2: The basic questions (Baclawski et al, 2020b)

so that it can be correctly searched for and employed as required by the FAIR principles.

What. This dimension is concerned with the specific details of the disruption. From an ontological perspective, this is the domain of the disaster. The biomedical domain is especially important because of the on-going COVID-19 pandemic as well as pandemics in general that have wide-ranging impacts on virtually everyone as discussed in Section 3. There are other aspects of health that can also have significant impact on the well-being of people, including nutrition and trauma (West, 2022; Fox, 2022; Dougherty, 2022). The environmental domain is another important source of disasters that have the potential for global impact. Climate change is a global emergency that has the potential to be a major disaster on many fronts; indeed, climate change is already having disastrous effects. Other environmental disasters include wildfires, floods (both of which are related to climate change), earthquakes, and volcanic eruptions. See Section 4. Monitoring the environment makes use of many types of sensors. Satellites are critically important for environmental sensing and are increasingly

important for many essential services such as internet communication and navigation as discussed in Section 5. Large constellations of satellites have now been deployed and are continuing to be deployed that have their own vulnerabilities and potential for disasters. Outer space beyond the immediate vicinity of Earth is yet another source for potential disasters, affecting communications from space weather-driven solar flares as well as losses from potential asteroid and comet impacts (Hull, 2022).

Why. An explanation is the answer to the question “Why?” as well as the answers to follow-up questions such as a request for technical details. Accordingly, explanations generally occur within the context of a process, which could be a dialog between a person and a system or could be an agent-to-agent communication process between two systems (Baclawski et al., 2020a). Explanations and justifications are important during all stages of a disaster. Prior to a disruptive event, planning requires the allocation of resources, and explanations are necessary to make a convincing case. When an emergency is developing into a potential disaster and after the emergency has resulted in a disaster, explanations are needed for raising awareness to prevent the disaster or to recover from it. The words, phrases and metaphors used for the explanations will determine the narrative, and if poorly chosen can hinder responses. For example, if the cause of a pandemic is perceived as being an infectious disease, then people will use a “war” metaphor in which the infectious agent is regarded as the “enemy” that must be “fought” and “defeated”. In fact, a pandemic is better regarded as being the result of issues such as human behavior and information failures, which are better described using very different terminology and metaphors.

How. By definition, “how” is concerned with the way something is done or happens. A complex event happens in a progression of stages called its lifecycle. The lifecycle of a disaster can be divided into stages: inactivity, onset, occurrence, recovery. The occurrence stage, such as in a wildfire, is generally referred to as “the disaster”. The onset progresses through various levels of severity leading up to the point where it is clear that a disaster is in progress. The occurrence stage can have more than one “wave” as the severity waxes and wanes. In practice, the division between the various stages of a disaster will only be known in retrospect and will differ from one region to another. Disaster management also has a lifecycle that is divided into anywhere from three to five stages or phases, depending on the particular management framework. The stages overlap one another,

and different sources list the stages in different orders. The most commonly mentioned stages are: prevention, mitigation, preparedness, response, and recovery. The UNDRR defines all of these terms (UNDRR, 2022). *Prevention* consists of activities and measures to avoid existing and new disaster risks. *Mitigation* is the lessening or minimizing of the adverse impacts of a hazardous event. *Preparedness* consists of the knowledge and capacities developed by governments, response and recovery organizations, communities and individuals to effectively anticipate, respond to and recover from the impacts of likely, imminent or current disasters. *Response* consists of actions taken directly before, during or immediately after a disaster in order to save lives, reduce health impacts, ensure public safety and meet the basic subsistence needs of the people affected. *Recovery* is the restoring or improving of livelihoods and health, as well as economic, physical, social, cultural and environmental assets, systems and activities, of a disaster-affected community or society, aligning with the principles of sustainable development and “build back better”, to avoid or reduce future disaster risk.

Another important management activity is hazard monitoring. The purpose of hazard monitoring is to achieve a state of readiness based on answering the basic question words for the hazard, such as: When, why and how may a hazard occur? Who would be affected? What are the warning signs? How do we minimize risk?

Who and Where. Disasters have a geographic extent where they occur, and the individuals who are affected are usually the ones living there. While the popularity of international travel has blurred the distinction between who and where, they are still closely related as disaster dimensions. The extent may range from a single individual to the entire world. A disaster for an individual may be an illness or trauma (Dougherty, 2022). An accident could involve just a few individuals. Local disasters can affect a city or a small region, such as epidemics, floods, wildfires and earthquakes (Fox, 2022; Jones and Moe, 2022; Berg-Cross and Sharma, 2022). Responses to disasters are generally at the national level even when a disaster is global. Global disasters include pandemics (Section 3), climate change (Section 4), and space disasters (Section 5). In all cases, geographic and geospatial information is critical in dealing with disasters.

When. The temporal span of a disaster has more than one aspect. The length of time can range from an hour or less to several millennia, and

the onset of the disruption can be sudden or gradual. Yet another aspect of when is the phase of the lifecycle of a disaster. Pandemics generally develop relatively suddenly but can last for only a few years or for thousands of years. There are three major ongoing pandemics, where a major pandemic is one that has around one million or more fatalities per year. COVID-19 lasted two years before most nations achieved some degree of control. The HIV pandemic has lasted forty years so far. The Tuberculosis pandemic has lasted at least 6000 years (Baclawski, 2022). By contrast, the onset of climate change has been very gradual, and the impact will last for centuries. Other environmental disasters, such as floods and wildfires can be very sudden but also are relatively brief. Space related disasters, such as solar flares are very sudden but brief, while asteroid impacts are now highly predictable, so they no longer have a sudden onset. In general, the timeliness of sensing events and sharing the what and where of disasters is critical.

Whither. After a disaster has ended, the prudent course of action is to take steps to ensure that one is prepared so that similar emergencies do not escalate to become disasters. Unfortunately, it is common for governments to ignore the problem once the disruption is over and public interest has waned. The metaphor that determines the narrative of a disaster, whether explicitly or implicitly, will affect public attitudes. For example, the “war” metaphor for a pandemic that is ending would encourage people to return to “pre-war” behaviors now that the “enemy” has been “defeated”. A more appropriate response would be to begin preparing for the next emergency (which may be seasonal) by permanently changing behaviors and by building a better information infrastructure. An example of a good response to a disaster is the UK Digital Twin project (West, 2022), and there are many examples of projects that are developing proactive interventions to prevent disasters for public health (Lieberman, 2022; Churchyard, 2022; Gil, 2022), the environment (Section 4), and space (Section 5).

Risk. Disasters and risks are fundamentally related notions. Risk assessments are necessary for planning purposes to prevent disasters, for monitoring and mitigating the effects of a disaster, and for recovering from a disaster. Generally, cost-benefit analyses based on risk assessments are the basis for choosing the most effective means of dealing with disasters at every stage. In addition to overall risk assessments, it is also important to

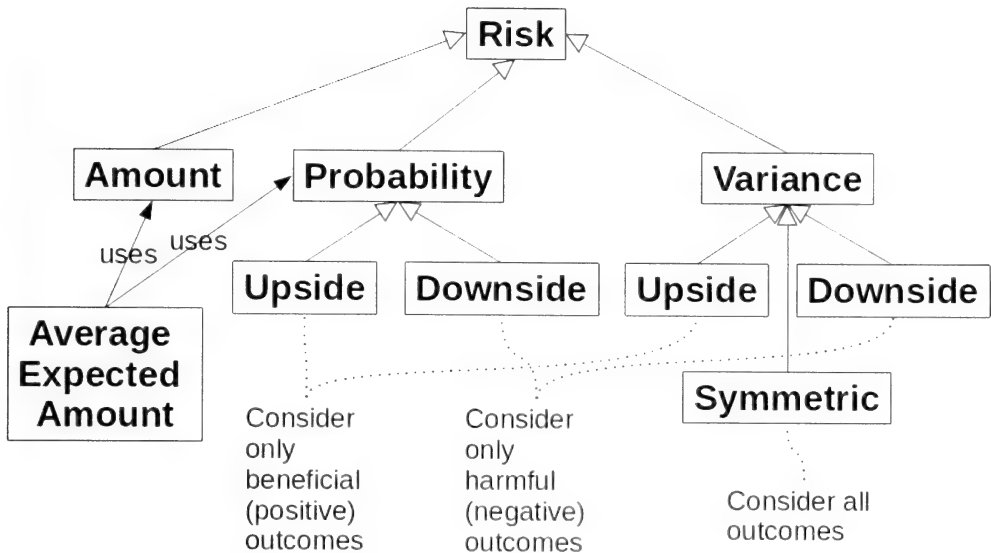


Figure 3: Taxonomy of Risk (Baclawski, 2022)

inform individuals about the risks associated with their behaviors. However, there are many interpretations of risk, and miscommunication can occur if different interpretations are conflated. The taxonomy of kinds of risk is shown in Figure 3 (Baclawski, 2022).

Severity. The number of individuals who have been injured or died as a direct result of a disaster as well as the cost due to the destruction of infrastructure and property are important dimensions of a disaster; however, these are complex statistics. They vary over time and can be difficult to measure. Some jurisdictions may be reluctant to report cases or may have differing criteria for their reports. For some disasters, such as hurricanes, it is even possible for estimated net fatalities to be negative. This happens because the fatality rate during the disaster can exceed the average mortality rate for the affected region. In addition, most disasters also have their own domain-specific measures like wind-speed for hurricanes, depths for floods and snowstorms and extent for wildfires.

Supply Chains. Although the term “chain” suggests a linear sequence of activities, a supply chain is often a complex network of organizations, people, activities, information, and resources. Responding to a

disaster usually requires supply chains for products and services, and a disaster can disrupt supply chains (Gil, 2022; Lieberman, 2022; Churchyard, 2022). For example, the COVID-19 pandemic required the creation of supply chains to provide vaccines, and the pandemic supposedly disrupted many supply chains. While there is evidence that the COVID-19 pandemic was one of the causes for supply chain disruptions, it is possible for supply chain disruptions to occur without any proximate cause because the supply chains can be dynamically unstable. This is known as the “bullwhip effect” (Section III, Baclawski et al, 2019).

Because a disaster is both affected by and affects supply chains, the disaster should be modeled as one of the components of the network. A further complication is that monitoring a supply chain (or any phenomenon) can affect the supply chain. This is known as the observer effect (Baclawski, 2018). To avoid observer bias, one should include monitoring processes as components in the network. The result of combining multiple supply chains, the disaster itself, as well as the monitors, in a network would require one to build and analyze a large, complex network. An important issue with complex networks is the need for interoperation and harmonization among components. Ontologies can help planners to model, analyze and monitor complex supply chains that affect and are affected by a disaster.

FAIR and TRUST. The degree to which information and semantic technologies relevant to a disaster conform to the FAIR and TRUST principles is an important dimension. When FAIR principles are not followed, disaster-related decision making can be very time-consuming because so much effort is required to acquire and to process the information that is necessary for a decision (Gil, 2022; Lieberman, 2022; Churchyard, 2022). Unfortunately, a recent survey of disaster management ontologies found that FAIR principles are seldom followed (Mazimwe, Hammouda, and Gidudu, 2021). The average Findability level was only 1.8%, the average Accessibility level was only 5.8%, and only 4.3% of the retrieved ontologies detail explicit mapping/correspondences between ontologies. Examples of disaster management projects that are based on ontologies conforming to the FAIR principles are described in Section 6.

3. Health Disasters

Health-related disasters span various landscape dimensions. For ex-

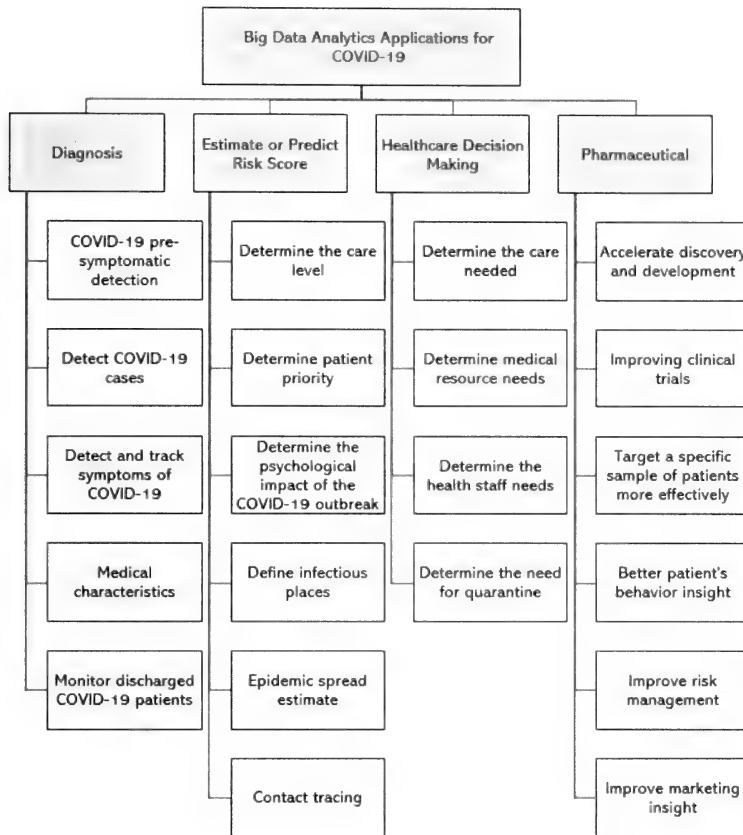


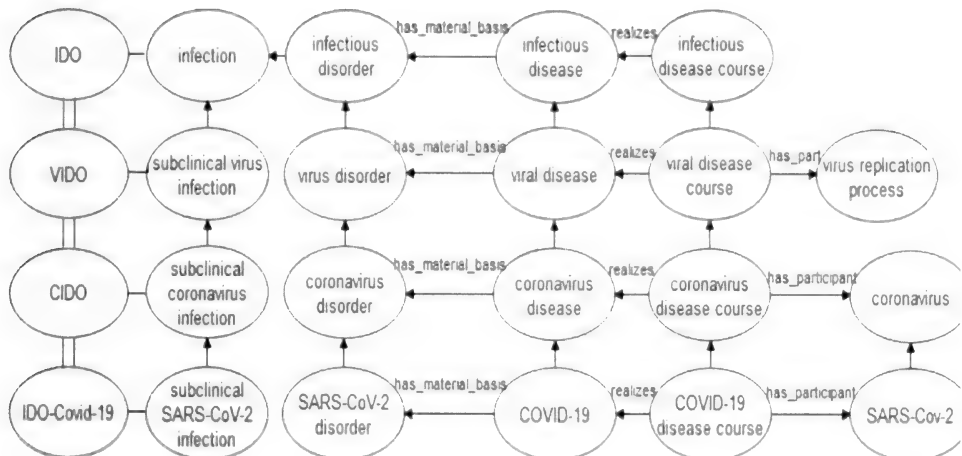
Figure 4: Taxonomy of COVID-19 Analytic Techniques
(derived from DeBellis and Dutta, 2021)

ample, different diseases can affect different groups of people (i.e., who and where), and health emergencies can be short-term or long-term (i.e., when). In most cases, the onset of a health-related disaster will be relatively sudden. Health disasters significantly affect and are affected by supply chains. A substantial range of data resources and information generally be needed for situational understanding of health-related disasters. The COVID-19 pandemic caused a large number of human fatalities as well as considerable havoc in the economic, social, societal, and health systems around the world. Responding to the pandemic was a major challenge. One aid to response was the varied use of an unprecedented amount of big data derived from public health surveillance, including vast amounts of real-time

monitoring of outbreaks, news reports, and organizational briefings. Some of the scope of the domain is shown in Figure 4. Much of this data was represented and stored using traditional data approaches, and websites offered a large, static representation of COVID-19 data. A limiting factor is that much of such data is largely unstructured (e.g., text, audio, video, image, newspaper, and blogs). This creates a major analysis and data integration problem. The data integration task gets simplified by the use of semantic technologies and the incorporation of knowledge organization systems (e.g., taxonomy, vocabulary and ontology) as background knowledge. Such resources fall along the semantic spectrum from controlled vocabularies to facilitate communication and understanding to linked data or structuring of data into easily queried knowledge graphs. Together these help meet the requirement for rapid data gathering and storage, but also results in COVID-19 data being stored across distributed geographies and often siloed databases. Such data siloing hinders translational and comparative research as well as slowing prognostic public health research needed in a time of a pandemic. For all these reasons, semantic technologies can help meet the challenge by supporting meaning-based data sharing across multiple disciplines and varied data systems.

Of particular interest is the use of formal, possibly openly available ontologies with well-specified syntax including a common space reachable by means of identifiers. One example of this is the adaptation of the Infectious Disease Ontology (IDO) made up of an aligned suite of interoperable ontology modules. These include ChEBI for chemical entities, Human Phenotype Ontology for human host phenotypes, and the more general Disease Ontology. Together these were designed to provide broad coverage across various aspects of the infectious disease domain. The IDO design was flexible to allow building new pathogen-specific ontologies in a simple way in order to allow novel disease data to be easily analyzed. This may take place in part by comparison to other pathogens, diseases and treatments. Using this knowledge an IDO implementation could help identify drug candidates that could be repurposed for an effective and safe COVID-19 treatment. Over 90 chemicals, drugs and antibodies against human coronavirus diseases were identified early on by mapping anti-coronavirus drugs to ontology IDs from ChEBI and drug data using semantic similarity analysis (Liu, et al. 2020). To do this for COVID-19 some parts of the core IDO model were enhanced by introducing the termed concept acellular which is a term

that covers viruses along with other acellular entities that are part of the study of virology. This term allowed one to distinguish infectious agents (i.e., organisms with an infectious disposition) from infectious structures (i.e., acellular structures that have an infectious disposition).



Relationships among IDO, VIDO, CIDO, and IDO-Covid-19 from Patel, Archana, et al. 2021.

Figure 5: Mapping relationships among biomedical ontologies

Three new IDO extensions were developed. The IDO Virus Ontology (VIDO) extended IDO to deal with viral infections (Babcock et al, 2021). The Coronavirus Infectious Disease Ontology (CIDO) extended VIDO for coronaviruses (He et al, 2022). Finally, CIDO was extended for COVID-19 cases and patient information with the CODO ontology, also called the IDO-Covid-19 ontology (Dutta, 2020; DeBellis, 2022; Dutta, 2022; DeBellis and Dutta, 2021). Relationships between these ontologies are summarized in Figure 5 which makes an essential point that modular ontologies may be aligned and work together using common concepts, such as exposure to COVID-19 and vital signs relevant to COVID-19, to cover portions of a domain of interest as needed and enabling broad querying among all the modules (Dutta and DeBellis, 2020). The work also illustrates the incremental way that modular ontologies may be matured (Berg-Cross, 2021c).

We have described some of the work on COVID-19 to help ensure

FAIR principles as well as to promote understanding. Among other things, this work shows the effectiveness of modular ontologies working together, expanding and harmonizing to support other technologies such as knowledge graphs.

4. Environment Disasters

Improving environment disaster management and recovery techniques is a priority given their impacts and given trends such as increased floods, droughts and the impact of climate change. One impediment to achieving improvements is the many definitions of environmental terms. There are, for example, many definitions of wildfires and floods.

As is true of other disasters. environmental disasters need rapid, flexible, but deep situational awareness, and have big data and analytic challenges arising from data heterogeneity and complexity, isolation and lack of conformity to FAIR principles. The situational awareness driver to reduce ambiguity and improve predictions is to mix historical data (e.g., prior cholera outbreaks that may have affected regional vulnerabilities before a hurricane makes landfall) with real-time data. One challenge is to effectively capture the status information and structure in a way that effectively improves situational awareness using diverse types of information from diverse sources as soon as it becomes available. There have been ontologies developed for disasters such as floods (Sinha and Dutta, 2020). Most of these ontologies are task ontologies that are formal, modular and use the Web Ontology Language (OWL) for their representation. The most used and reused are the Semantic Web for Earth and Environmental Terminology (SWEET) ontology, the contextual design patterns of the Semantic Sensor Network (SSN) ontology, and ontologies for Time and Space. In general, the domain of flooding remains only lightly formalized.

As with the previously described COVID-19 work, knowledge graphs help handle some of the data silo problems by acting like a default common data model. Knowledge graphs, like ontologies, emphasize structuring relationships along with attributes. For more about knowledge graphs and their connections with ontologies see (Baclawski et al, 2020b).

Until recently, knowledge graphs were not very successful in the realm of environmental data and environmental intelligence. This was in part because spatial data requires special treatment and because of the

difficulty of usefully lifting environmental data to a knowledge graph using formal semantics.

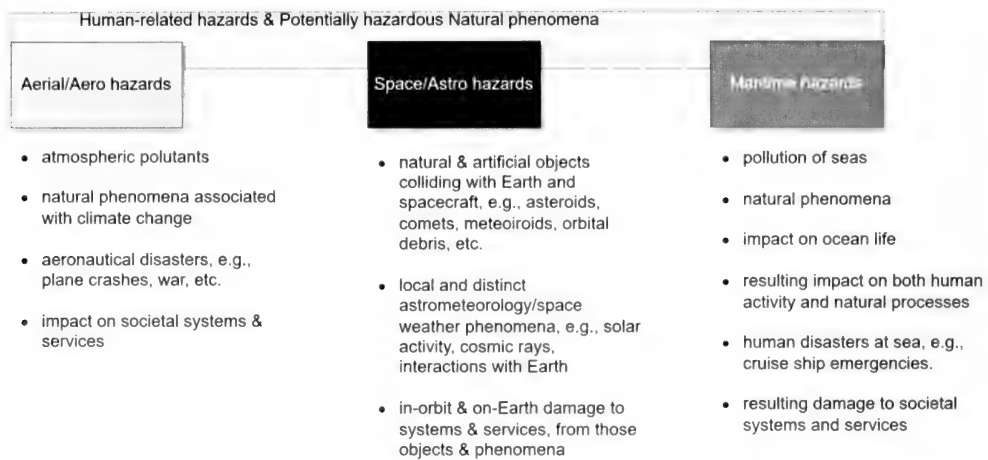
Fortunately, for the past 50 years the Earth science community has been establishing its infrastructure not only for current space-based image data required for monitoring the disasters but also for changes in the environment over the years (Sharma, 2022b). Semantics, metadata, sensors and platforms as well as repositories enable search and discovery tools, and communities are increasingly being formed to address timeliness and relevance of data for disaster management support. Harmonization of data and metadata, and use of diverse platforms from NASA, NOAA, ESA and other agencies is being increasingly sought and some ontologies addressing overlap areas are being developed (Sharma, 2022a; NASA, 2018). Agencies (e.g., UNDRR, FEMA) and communities (e.g., the Earth Science Information Partners (ESIP)) play increasing roles in monitoring and mitigation.

5. Aerospace and Maritime Disasters

As with health-related and environmental disasters, aerospace and maritime disasters can be characterized by the basic questions and the risk, severity and supply chain dimensions. The diagram in Figure 6 classifies disasters for aerial, maritime and outer space situations. The common thread is a distinction between human-associated hazards or activity, and natural phenomena that may potentially result in disasters. Note that the various hazards overlap with one another.

Aeronautical and atmospheric hazards and disasters include artificial pollutants impacting the atmosphere and affecting the health of living creatures, natural phenomena possibly associated with climate change, airplane crashes, as well as human conflict activities such as war, crime, terrorism, etc. Disasters in this context may have harmful impacts on systems and services in societies, which overlaps with arguably any sort of potential disaster and context. For each, there is associated research, and investigative, activities that have collected various sorts of data (EPA, 2022).

Maritime hazards include artificial pollution of the seas and debris (NOAA, 2022), which can harm both human and non-human life (Avakian, 2022), thereby impacting natural processes and ecosystems; natural phenomena, whether associated with human activity or not; human emergen-



By Robert J. Rovetto | <https://ontospace.wordpress.com/contact> | rrovetto@terpalum.umd.edu
 Contact for diagram services: <https://tinyurl.com/diagramsRov>

Figure 6: Classification of Aeronautical, Maritime, and Space Hazards (Rovetto, 2022)

cies at sea, such as cruise or cargo ship disasters; as well as any resultant damage to systems and services in societies. Like the aeronautical context, both data-centric research is conducted for changes in marine ecosystems, and data is collected for investigations into human disasters at sea.

Space hazards can come from both artificial and natural phenomena but are different in some respects from aeronautical and maritime hazards. The main kinds of space hazards are meteoroids, debris (NASA, 2022a), and solar flares. Smaller meteoroids are difficult to track although the technology is improving. The impact of a meteorite is literally its impact with the Earth. Space debris near Earth is now being tracked and can potentially be mitigated by preventing its creation through appropriate spacecraft design and debris removal measures. Like meteorites, space debris will impact the Earth, but can also impact spacecraft (NASA, 2016), which could harm astronauts as well as the financially expensive technological systems and the services they provide, with a significant impact on society. For example, loss of artificial satellites due to debris may result in damage to Global Positioning Systems, negatively impacting navigation on Earth. Similarly, so for the loss of communications services, internet services, observational services (scientific, military, etc.). A collision between orbital debris and

other satellites would produce more debris which could cascade to render near Earth space activities impossible for decades, a phenomenon known as the Kessler syndrome (Hull, 2022). Extreme space weather, especially solar flares, is another kind of space hazard (ESA, 2022). The potential impact is on space-based and terrestrial communication and power systems (NOAA, 2023).

Given the active and diverse areas of big data research and given the need for data collection when investigating disasters such as those described above, knowledge organization systems (such as NASA, 2022b), including ontologies, could play a useful role. A space domain reference ontology is presented in Section 6.

6. Project Examples

In this section we summarize some of the projects that have been developing and using ontologies for disaster monitoring and response management.

VIDO, CIDO and CODO. VIDO extends the IDO ontology to add virus-specific entities and provides concrete information about the domain of virus disease. In particular, VIDO specialized the IDO concepts by addition of the term “virus” to create a subclass. Using what was known of the viruses the logical relations and textual information about the classes were ontologized. For example, as shown in Figure 5, IDO’s Infectious Disease became Viral Disease. The latest version of VIDO was released in August 2020 (Babcock et al, 2021).

The CIDO ontology further specialized VIDO with coronavirus disease concepts. CIDO is a community-based, open source ontology that is interoperable with other existing Open Biological and Biomedical Ontology (OBO) Foundry ontologies. CIDO has imported terms from over 30 OBO Foundry ontologies, including all SARS-CoV-2 protein terms from the Protein Ontology, COVID-19-related phenotype terms from the Human Phenotype Ontology, and over 100 COVID-19 terms for vaccines from the Vaccine Ontology. CIDO has been used in various applications such as term standardization, inference, natural language processing (NLP), clinical data integration and drug repurposing for COVID-19 treatment (He et al, 2022).

The community based CODO ontology published on Bioportal has

4000 plus terms and was designed to capture particular data about the COVID-19 pandemic. The idea was to support the collection of epidemiological data starting with the representation of the novel corona viruses and variants along with phenotypes, anti-coronavirus drugs and medical devices (e.g., ventilators). An example of the part of the CODO ontology connected to a patient is shown in Figure 7 (Dutta, 2022).

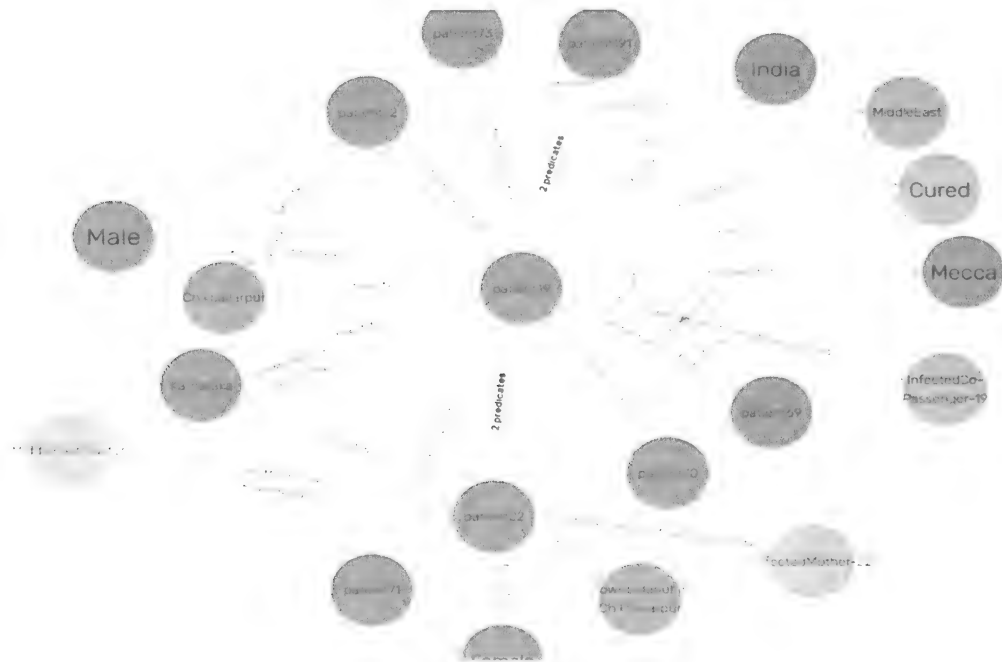


Figure 7: The part of CODO connected to a particular patient (Dutta, 2022)

The CODO ontology, available on the CODO Github (Dutta, 2020), was designed by analyzing disparate COVID-19 data sources such as datasets on cases, patients, relations (e.g., family, co-workers), and on the COVID-19 Data Repository at Johns Hopkins University. Geographic locations and date-time information was also available. CODO leveraged literature and services information, and its coverage includes contact tracing, diagnosis, disease measures, comorbidity, treatments and drugs, vaccination, cases and resource descriptions, tests, and preventive measures, along with responses and relevant contextual influences such as weather situations. To adapt to COVID-19 challenges a health facility concept had

to be a sub-type as, for example, a COVID-19 dedicated facility which is further sub-categorized into COVID-19 care center, dedicated COVID-19 health center, and dedicated COVID-19 hospital. To facilitate its use by data and service providers, CODO was published using FAIR principles. The ontology has been used by several projects. For example, it has been used as a metadata enhancer to annotate COVID-19 literature, and for COVID-19 risk detection system which can help with COVID-19 contact tracing (Lin et al, 2021).

The value of the CODO ontology was demonstrated by using it to build knowledge graph using an agile approach in just a few months. The resulting knowledge graph had approximately 5M triples and allowed tracking cases with information about traveling companions. Taken as a whole the experience demonstrates some common principles that apply to the process of scaling up from an ontology model to a knowledge graph with real-world data and how resources get expanding and harmonizing to support other semantic resources like knowledge graphs (DeBellis and Dutta. 2021). Knowledge graphs, as discussed in “Ontology Summit 2020 Communiqué: Knowledge Graphs,” are a novel paradigm for the representation, retrieval, and integration of data from highly heterogeneous sources. Within just a few years, knowledge graphs and their supporting technologies have become a core component of modern search engines, intelligent personal assistants, business intelligence, and so on (Baclawski et al, 2020b).

OGC Pilot. This Open Geospatial Consortium (OGC) Disaster Pilot 2021 (D21) uses a health spatial ontology for disaster response management. The goal of D21 is to develop standards-based services to support rapid decision making through the full lifecycle of disaster management for multiple hazards. D21 includes details for impacted entities, such as the affected individuals, vulnerable individuals (e.g., chronically ill and disabled persons), and the transportation infrastructure, both land and air. The objective is to ensure that the supply chains can adequately supply the pilot study area even when there is a disaster. For example, vaccines must be available to inhibit the spread of a disease, trauma treatment may be needed due to sudden floods. It is also necessary to prevent individuals from being victimized, losing personal effects, spreading other pathogens, etc. The pilot is a multi-layered thematic data approach and a conceptual model that is implemented using an ontology conforming to the FAIR principles (Churchyard, 2022; Lieberman, 2022).

D21 was applied during a flood disaster in the Peru - Rimac River Basin. The medical supply needs map uses a detailed workflow of the required and available supplies and includes a geospatial mapping of provider and supplier facilities and available inventory. D21 was also applied to a hospitals and medical supplies scenario in New Orleans, Louisiana. Future work and applications of the team at HSR.Health (Healthsolutionresearch.org) are planned to include more studies of other disasters where response management depends on supply chains (OGC, 2021; 2022; Lieberman & Voidrot, 2021).

Smart Cities. The Smart Cities Working Group Report is based on foundational, citywide ontologies to address public health emergency service levels. The ontologies can be updated by one agency but can be read by multiple agencies. Entities have been defined and a dozen patterns have been developed that address concepts such as person, government and vaccination. Correlation matrices among patterns, and pattern-based disaster-related use cases have been developed. Other techniques that have been employed include micro theories and knowledge graphs (Fox, 2022).

Unfortunately, legacy systems can create disaster data silos across the departments/divisions/areas dealing with disasters. A first step to breaking down the silos is the creation of data standards, but sharing also requires harmonization without which a standard may become a hindrance because it is not trusted (Berg-Cross, 2021a, 2021b).

KnowWhere Graph. The KnowWhere Graph (KWG) is a spacial knowledge graph system that can quickly answer questions such as “What is here?”, “What happened here before?”, “Who knows more?”, “How does it compare to other regions or previous events?”. Situational awareness is enhanced by continually adding content and by using tools such as Environmental Systems Research Institute, Inc. (ESRI) GeoEnrichment. To overcome some shortcomings of knowledge graphs, they are combined with GeoEnrichment to form the KWG. Examples of applications include the Farm to Table Supply Chain and Sustainability Project. The KWG has reduced uncertainty for pandemic risk analyses. The KWG is currently a knowledge graph with over 10 billion edges. Examples of future challenges include spatiotemporally explicit knowledge graph embeddings that are invariant under syntactic changes (Janowicz, 2022).

A particular feature of the KWG effort is the process by which

data becomes augmented using a range of auxiliary data and information adapted as needed to a geospatial study area. A simple example is mapping demographic data to the various ways that regions are represented. geoenrichment tools can significantly reduce the costs involved in acquiring, entering, and cleaning geo-data (Vockner and Mittlböck, 2014). However, until very recently, pre-knowledge graph approaches for geoenrichment were expensive, only used pre-defined categories of information to access data and were not effective in supporting the data integration or interoperability requirements of the FAIR principles (Janowicz et al., 2022). The KWG project supports a FAIR approach with data-driven decision-making and data analytics that address previous weaknesses of AI-based technologies, together with an open, cross-domain knowledge graph.

MINT. The Model Interventions (MINT) project is modeling complex human-nature systems for disaster preparedness and response. The natural disasters being studied are floods, food insecurity and drought. The goal is to use multiple interoperable models and AI to reduce the time required for making decisions for interventions from years to weeks. The impacts of many types of potential interventions can be modeled, such as reducing the fertilizer price or recharging the aquifers to ensure food security. Interventions are to indicate results, costs, risks, and baselines in this framework. Future work will incorporate uncertainties in models and sensitivity analyses of variables (Gil, 2022).

PLACARD and weAdapt. The PLAtform for Climate Adaptation and Risk reDuction (PLACARD) project seeks to support the coordination of climate change adaptation and disaster risk reduction communities (Barrott, Bharwani and Brandon, 2020). PLACARD is an EU Horizon 2020 (H2020) project that is working to change the basic organizational information and knowledge management (IKM) practices to accelerate action on climate change and to reduce impacts. The weAdapt project grew out of the PLACARD experience (Bojovic, Giupponi and Karali, 2017). Previous efforts to classify, categorize and structure climate-relevant knowledge as needed have not achieved FAIR data organization in the face of dynamic data acquisitions and have failed to leverage all information available or to reach intended audiences in a useful way. As a result, it has not been possible to easily and rapidly find, reuse and share relevant information (Barrott and Bharwani, 2022). When information can be found, it is often difficult or impossible to understand it, and thus it cannot be used (Zuccaro and

Martucci, 2020). WeAdapt aims to provide FAIR data and understanding by developing some high level knowledge management structures such as standard topic areas and taxonomies but also practices and standards (Pulquério, 2017).

I-ADOPT. The InteroperAble Description of Observable Property Terminologies (I-ADOPT) is another project concerned with developing FAIR environmental information, but worked at a lower level than weAdapt, on vocabularies and might be seen as a complementary effort that could be leveraged by weAdapt. I-ADOPT is a community effort to develop a harmonizing framework to address the I in FAIR for discussing and representing climate topics. I-ADOPT started by gathering a series of use cases from the environmental science community. These were compiled and analyzed using a catalog of existing vocabularies and conceptual models. Using the results, the I-ADOPT community determined at a high level the minimal viable set of components and relationships needed to describe the variables and parameters of the various communities within and across environmental science domains. It was expected that annotation of current observable property standards using the FAIR vocabulary components of the I-ADOPT framework would aid in increasing interoperability across the wide variety of data standards within the environmental science domain (Magagna et al, 2022; Magagna and Schindler, 2022).

In particular, I-ADOPT represents the high level concepts of WHAT has been observed independently of WHERE, HOW and WHEN the data acquisition took place. Environmental examples include identifying wind speed (vs. speed of wind), soil color (vs. color of soils), concentration of atomic nitrogen in Earth's atmosphere (vs. nitrogen concentration). Of conceptual importance, the I-ADOPT Ontology builds on the high level framework by using a design pattern that adds the concept of matrix and its relations to entities, properties and constraints. The overall benefits of the I-ADOPT vocabulary include:

1. Supporting interoperability between existing terminologies
2. Enabling semantically precise and FAIR descriptions of variables
3. Decomposing descriptions into atomic components and linking those to existing vocabularies making these descriptions of observed variables machine-actionable

- 4. Providing abstract reusable semantic descriptions for concrete observations
- 5. Enabling mappings between variable descriptions across terminologies
- 6. Requiring no change to existing structures
- 7. Adding rich (human-readable and machine-actionable) descriptions with qualified references
- 8. Boosting Findability and Reusability of data

Satellite Teams. One of the most important services of near-Earth artificial satellites is for environmental sensing. There are well over 100 active government-sponsored Earth observation satellites, as well as around 40 active commercial Earth observation satellites. Within this large collection, there are constellations of satellites that cooperate to improve their observations by fusing their data. A prominent example is the A-train, currently consisting of three satellites: OCO-2, GCOM-W1 and Aura. The collective observations of A-train satellites are being used to build high-definition three-dimensional images of Earth's atmosphere and surface. Achieving such cooperation requires data harmonization so that the observations of the satellites can be fused to form common observations. Common data formats and available metadata are important for this process (Sharma, 2022b).

OSEDO. The Orbital Space Environment Domain Reference Ontology (OSEDO) suite is a set of ontologies and other semantic resources to support astronomical and astronautical data, research, science, activity and interdisciplinary activities (O'Neil and Rovetto, 2021; Rovetto, n.d.; Rovetto, 2016). The suite includes the Orbital Debris Ontology (Rovetto, 2015), Space Situational Awareness ontology (Rovetto and Kelso, 2016), Astronomical Environment ontologies, and the Astrometeorology/Space Weather Ontology, among others. Example applications in the suite include interactive 3D orbital systems. These ontologies serve as conceptual models, sources for terminology, and formal representations of the target topic areas. They aim to provide metadata to annotate data and documents associated with relevant topics, as well as definitions and formal

semantics. Some of the activities supported by OSEDO include conceptual analysis, concept clarification, developing and offering vocabularies, modeling for various stakeholders, exploring terminology synchronization and semantic harmonization for the respective disciplines and stakeholders, and multidisciplinary collaboration and innovation (NASA, 2019). Future services will include ontology-assisted space debris and collision avoidance management. Within the discipline itself, removing harmful space debris is an active area of research that will make the orbital space environment safer for the global community (Rovetto, 2022).

7. Summary and Conclusion

The main findings in this article are:

1. Due to framing, terminology and metaphors can have unanticipated, negative effects on disaster response. It is important for disaster relief agencies to be careful to choose the terminology and metaphors and to control the narrative in outlets such as social media as well as to ensure the proper use of relevant information (Stickles, 2019).
2. The root causes from whence a disaster arises are often misunderstood or misrepresented. The root causes of the COVID-19 pandemic were information and behavioral failures, not the disease, which was the immediate, proximate cause.
3. Explanations can be a useful tool for disaster management, but they must be in the form of an interactive dialog rather than simple flat answers (Baclawski et al., 2020a).
4. There are many interpretations of risk, with the main split being between risk as a probability and risk as a variance. Clarifying the intended interpretation would help prevent misunderstanding. Ideally, it would be best to use full probability distributions, or at least both the probability and the variance.
5. Work is still needed to make semantic resources and knowledge organization systems compliant with FAIR and TRUST principles.
6. We have observed that there are cross-disaster linkages among kinds of disasters; for example, environmental disasters impacted pandemic

patients, its spread and supply chain routes required to care for the patients. The landscape dimension framework developed in Section 2 was intended to help identify cross-disaster linkages and to find opportunities for reusing ontologies and other information resources, but more work needs to be done to realize this potential.

With regard to health disasters, work still needs to be done to incorporate heterogeneous data concepts; for example, “long COVID” for the COVID-19 pandemic and “close contact” for different diseases and variants. Moreover, incorporating heterogeneous data concepts should be done in a way that provides deeper harmonization between not only the data, but also the metadata as found in glossaries, e.g., (Penn, 2022) and other semantic technologies. As in many knowledge engineering efforts, access to the best suite of domain experts is a limiting factor, especially during emergencies.

While there is much we now know about developing knowledge graphs for environmental disasters, there is much more to learn as we blend the role of classical knowledge representations with the machine learning (ML) approach of knowledge embeddings. A hybrid approach seems like an important part of future work as more reasoning is enabled as part of a knowledge graph. Key research questions include how to incorporate spatiotemporal and commonsense reasoning, how to learn and support geographic knowledge graph summaries that are meaningful to users, how to quantify and represent regional differences, and how to detect and mitigate bias in geographic knowledge graphs.

Acknowledgments

Certain commercial software systems are identified in this paper. Such identification does not imply recommendation or endorsement by the National Institute of Standards and Technology (NIST) or by the organizations of the authors or the endorsers of this article; nor does it imply that the products identified are necessarily the best available for the purpose. Further, any opinions, findings, conclusions or recommendations expressed in this material are those of the authors and do not necessarily reflect the views of NIST or any other supporting U.S. or European governments or corporate organizations.

We wish to acknowledge the support of the ontology community,

especially the invited speakers and participants who contributed to the Ontology Summit 2022, which was the primary basis for this article. Thanks to the NIST reviewers— Spencer Breiner and Paul Witherell – for their detailed review of the document, and to Aliza Reisberg for Figure 1. There were many invited speakers, some of whom gave presentations at more than one session. The complete list of sessions, speakers, and links to presentation slides and video recordings is available at (Ontology Summit, 2022).

References

Avakian, M. (2022). New Study Finds Ocean Pollution a Threat to Human Health, NIH. <https://bit.ly/3Aj7sgZ>

Baclawski, K., Bennett, M., Berg-Cross, G., Fritzsche, D., Sharma, R., Singer, J., Singer, J., Sowa, J., Sriram, R.D., Underwood, M., Whitten, D. (2020a). Ontology Summit 2019 Communiqué: Explanation. *Applied Ontology*. DOI: 10.3233/AO-200226 <http://bit.ly/2TDdyTG>

Baclawski, K., Bennett, M., Berg-Cross, G., Fritzsche, D., Sharma, R., Singer, J., Sowa, J., Sriram, R.D., Whitten, D. (2020b). Ontology Summit 2020 Communiqué: Knowledge Graphs. *Applied Ontology*, 16 (2), 229–247.

Baclawski, K., Chystiakova, A., Gross, K.C., Gawlick, D., Ghoneimy, A. and Liu, Z.H. (2019) Use Cases for Machine-Based Situation Awareness Evaluation. In IEEE Conference on Cognitive and Computational Aspects of Situation Management. <https://bit.ly/3PHKsxG>

Baclawski, K. (2018) The observer effect. In IEEE Conference on Cognitive and Computational Aspects of Situation Management (CogSIMA 2018). <https://bit.ly/3AiXwUy>

Baclawski, K. (2022) What is Risk? In Ontology Summit 2022. <https://bit.ly/3IfhQ2>

Barrott, J. and Bharwani, S. (2022) How to make knowledge interoperable: examples from weADAPT and the Connectivity Hub. In Ontology Summit 2022. <https://bit.ly/3NPPtVd>

Barrott, J., Bharwani, S. and Brandon, K. (2020) Transforming knowledge management for climate action: a road map for accelerated discovery and learning. PLACARD project, FC.ID: Lisbon.

Bennett, M. (2021). The Landscape of Ontology Purpose. <https://bit.ly/3rIs4K4>

Berg-Cross, G. (2021a). Introduction to Harmonizing Definitions and the EnvO Ontology. <https://bit.ly/3pnkwdG>

Berg-Cross, G. (2021b). Semantic harmonizations of concepts revisited: work in the context of the ontology development landscape. <https://bit.ly/3vsfJuY>

Berg-Cross, G. (2021c). Issues in Incrementally Adding Better Semantics to Knowledge Graphs. *J. Wash. Acad. Sci.* 107(3):33-58.

Berg-Cross, G. and Sharma, R. (2022). Overview of the Disaster Parameter Landscape and Environmental Disasters. In Ontology Summit 2022. (19 Jan 2022) <https://bit.ly/3trtHiT>

Bojovic, D., Giupponi, C., and Karali, E. (2017) Social Network Analysis of the PLACARD Project Stakeholders. <https://bit.ly/3PJXCuh>

Churchyard, P. (2022) Health Spatial Data Infrastructure - part of the OGC 2021 Disaster Pilot. In Ontology Summit 2022. <https://bit.ly/3trSWIg>

DeBellis, M., and Dutta, B. (2021) The COVID-19 CODO Development Process: an Agile Approach to Knowledge Graph Development, Iberoamerican Knowledge Graphs and Semantic Web Conference. Springer, Cham.

DeBellis, M. (2022) Semantic Technology and the COVID-19 Pandemic. In Ontology Summit 2022. <https://bit.ly/3v7VJkn>

Dougherty, A. (2022), Personal Emergency Management using the Free Life Planner. In Ontology Summit 2022. <https://bit.ly/36XZSxp>

Dutta, B., and DeBellis, M. (2020) CODO: an ontology for collection and analysis of COVID-19 data. arXiv preprint arXiv:2009.01210

Dutta, B. (2022) CODO: an ontology for collection and analysis of multiparadigm COVID-19 data. In Ontology Summit 2022. <https://bit.ly/3v7VJkn>

Dutta, B. (2020) CODO Github. <https://github.com/biswanathdutta/CODO>

EPA (2022). Hazardous Air Pollutants, U.S. Environmental Protection Agency, <https://www.epa.gov/haps>

ESA (2022). Space weather and its hazards, European Space Agency, <https://bit.ly/3QRgU1V>

Fox, M. (2022) ISO/IEC WG11 Data Standards for Public Health Emergencies and Related Ontologies. In Ontology Summit 2022. <https://bit.ly/3sGeNU1>

Gil, Y. (2022) Ontologies for Exploring Interventions for Disaster Preparation and Response. In Ontology Summit 2022. <https://bit.ly/3ubnvM0>

GO FAIR (2022). FAIR Principles. <https://bit.ly/3QGETRj>

He, Y., Yu, H., Huffman, A., Lin, A., Natale, D., Beverley, J., ... and Smith, B. (2022). A comprehensive update on CIDO: the community-based coronavirus infectious disease ontology, *J. Biomed. Semantics* 13: 25. <https://bit.ly/3szUyYn>

Hull, S.M. (2022) Potential Space Disasters, and What We Can Do to Prevent Them. In Ontology Summit 2022. <https://bit.ly/3r5SZ3Y>

IFRC (2022). What is a disaster? <https://bit.ly/3T8YzPr>

Janowicz, K., et al (2022) Know, Know Where, KnowWhereGraph: A densely connected, cross-domain knowledge graph and geo-enrichment service stack for applications in environmental intelligence, *AI Magazine* 43.1: 30-39.

Janowicz, K. (2022) Knowledge Graphs and Disaster Mitigation. In *Ontology Summit 2022*. <https://bit.ly/3r6wv2V>

Jones, D. and Moe, K. (2022) ESIP Cross-Domain Collaboratory: Challenges and Opportunities. In *Ontology Summit 2022*. <https://bit.ly/3u4Xz4t>

Lieberman, J. (2022) Overview of the OGC Disaster Pilot. In *Ontology Summit 2022*. <https://bit.ly/3trSWlg>

Lieberman, J., Voidrot, M.-F. (2021) Bringing Eyes in the Sky to Disaster Awareness on the Ground: OGC Disaster Pilot 2021. In Canadian Council on Geomatics December Meeting. <https://bit.ly/3KajxcN>

Lin, A. Y., Yamagata, Y., Duncan, W. D., Carmody, L. C., Kushida, T., Masuya, H., ... & He, Y. (2021). A Community Effort for COVID-19 Ontology Harmonization. In *ICBO* (pp. 122-127). <https://bit.ly/3fbocjH>

Lin, D., Crabtree, J., Dillo, I. et al (2020) The TRUST Principles for digital repositories. *Sci Data* 7, 144 (2020). <https://bit.ly/3pGBNBc>

Liu, Y., Chan, W.K., Wang, Z., Hur, J., Xie, J., Yu, H., He, Y. (2020) Ontological and Bioinformatic Analysis of Anti-Coronavirus Drugs and Their Implication for Drug Repurposing against COVID-19. *Preprints 2020*, 2020030413 (doi: 10.20944/preprints202003.0413.v1).

Magagna, B. and Schindler, S. (2022) How to make climate research interoperable with I-ADOPT from field observation to data publication. In *Ontology Summit 2022*. <https://bit.ly/3NPPtVd>

Magagna, B. et al (2022) InteroperAble Descriptions of Observable Property Terminologies (I-ADOPT) WG-outputs and recommendations. RDA endorsed Recommendations.

Mazimwe, A., Hammouda, I., and Gidudu, A. (2021) Implementation of FAIR Principles for Ontologies in the Disaster Domain: A Systematic Literature Review. *ISPRS Int. J. Geo-Inf.* 10, 324. <https://bit.ly/3wuUmvU>

NASA (2016). Space Debris: Understanding the Risks to NASA Spacecraft, National Aeronautical and Space Administration. <https://go.nasa.gov/3pIpeFg>

NASA (2018). Harmonized Landsat Sentinel-2. <https://hls.gsfc.nasa.gov/>

NASA (2019). Orbital Debris Ontology, Terminology, and Knowledge Modeling, <https://go.nasa.gov/3AIInnGV>

NASA (2022a). NASA ORBITAL DEBRIS PROGRAM OFFICE, National Aeronautical and Space Administration, <https://go.nasa.gov/3dJK4kX>

NASA (2022b). NASA Technology Taxonomy, <https://go.nasa.gov/3cqY0Qx>

NOAA (2022). Ocean pollution and marine debris, National Oceanographic and Atmospheric Association, <https://bit.ly/3PPbFyF>

NOAA (2023). Space Weather Prediction Center, <https://www.swpc.noaa.gov/impacts/>

OGC (2021). Disaster Pilot 2021. <https://bit.ly/3wlHpUW>

OCG (2022). OGC Data for Disasters User and Provider Readiness Guides. <https://bit.ly/3woTOYp>

Ontology Summit (2022). List of Speakers. <https://bit.ly/3wk6uzW>

O’Neil, D.A.; Rovetto, R.J. (2021). “An Ontology-Based Virtual Orrery,” NASA Technical Memorandum, 2017-2021, <https://go.nasa.gov/3ztqmSI>, Accessed 27 October 2022.

Penn (2022). The Glossary of COVID-19 Terms, University of Pennsylvania. <https://bit.ly/3AG6igV>

Pulquério, Mário (2017) PLACARD-Platform for Climate Adaptation and Risk reDuction-Horizon 2020 project, Impact 2017.3: 14-16.

Rovetto, R.J. (2015). An ontological architecture for orbital debris data, Earth Science Informatics. <https://bit.ly/3QS7nrs>

Rovetto, R. (2022), Space Hazards and Space Ontology. In Ontology Summit 2022. <https://bit.ly/3LNbQZL>

Rovetto, R.J. and Kelso, T.S. (2016). Preliminaries of a Space Situational Awareness Ontology, Advances in the Astronautical Sciences Spaceflight Mechanics, Volume 158. <https://bit.ly/3pJyfOt>

Rovetto, R.J. (n.d.). Orbital Space Domain Knowledge Modeling. <https://bit.ly/3NIWe15>, Accessed 27 October 2022.

Rovetto, R.J. (2016). The Orbital Space Environment and Space Situational Awareness Domain Ontology – Towards an International Information System for Space Data, Advanced Maui Optical and Space Surveillance Technologies Conference (AMOS).

Sharma, R. (2022a). Potential topics: Ontology and Disasters. In Ontology Summit 2022. <https://bit.ly/3RnNYz8>

Sharma, R. (2022b). Earth Observations to monitor disasters - sensors, platforms, image-data and metadata. In Ontology Summit 2022. <https://bit.ly/3uVXiAf>

Sinha, P., and Dutta, B. (2020) A Systematic Analysis of Flood Ontologies: A Parametric Approach, Knowledge Organization 47.2.

Stickles, E. (2019) MetaNet Metaphor Repository. <https://bit.ly/32g4u9Q>

UNDRR (2022). Disaster Terminology. <https://bit.ly/3ACu2m4>

Vockner, B., and Mittlböck, M. (2014) Geo-enrichment and semantic enhancement of metadata sets to augment discovery in geoportals, ISPRS International Journal of Geo-Information 3.1: 345-367.

West, M. (2022) Whence Disasters. In Ontology Summit 2022. <https://bit.ly/3v7VLJ1>

Zuccaro, G., Leone, M.F., and Martucci, C. (2020) Future research and innovation priorities in the field of natural hazards, disaster risk reduction, disaster risk management and climate change adaptation: A shared vision from the ESPREssO project, International Journal of Disaster Risk Reduction 51: 101783.

KENNETH BACLAWSKI is an Associate Professor Emeritus at the College of Computer and Information Science, Northeastern University. Professor Baclawski does research in data semantics, formal methods for software engineering and software modeling, data mining in biology and medicine, semantic collaboration tools, situation awareness, information fusion, self-aware and self-adaptive systems, and wireless communication. He is a member of the Washington Academy of Sciences, IEEE, ACM, IAOA, and is the chair of the Board of Trustees of the Ontolog Forum.

MIKE BENNETT is the director of Hypercube Limited, a company that helps people manage their information assets using formal semantics. Mike is the originator of the Financial Industry Business Ontology (FIBO) from the EDM Council, a formal ontology for financial industry concepts and definitions. Mike provides mentoring and training in the application of formal semantics to business problems and strategy, and is retained as Standards Liaison for the EDM Council and the IOTA Foundation, a novel Blockchain-like ecosystem.

GARY BERG-CROSS is a cognitive psychologist (PhD, SUNY-Stony Brook) whose professional life included teaching and R&D in applied data & knowledge engineering, collaboration, and AI research. A board member of the Ontolog Forum he co-chaired the Research Data Alliance work-group on Data Foundations and Terminology. Major thrusts of his work include reusable knowledge, vocabularies, and semantic interoperability achieved through semantic analysis, formalization, capture in knowledge tools, and access through repositories.

ROBERT J. ROVETTO is a formal ontologist and philosopher who has written over 20 articles and has participated in international standards development and the Ontology Summit. His focus areas include: terminology and knowledge representation; conceptual modeling; upper or foundational ontology; foundational concepts; ontology development methodology; ontology for space (<https://purl.org/space-ontology>), maritime, and emergency response; as well as ethics of/in ontology.

DR. RAVI SHARMA is a Senior Enterprise Architect, an industrial entrepreneur, theoretical nuclear and particle physicist, human space systems scientist, fuel cell and hydrogen technologies specialist, satellite remote sensing and image data systems specialist, an Enterprise Architect with SOA, BPM and modeling expertise and has several decades of computer systems and peripheral manufacturing and IT systems development experience. Dr. Sharma has received the NASA Apollo Achievement Award for his work on the NASA Apollo and Skylab Programs, where he helped select, analyze, build and design space and ground systems relating to remote sensing and spacecraft contamination analysis. He has also worked on the Space Station, Space Shuttle, Landsat, EOS (Terra, Aqua, Aura and NPOESS) satellites and ground systems.

RAM D. SRIRAM is currently the chief of the Software and Systems Division, Information Technology Laboratory, at the National Institute of Standards and Technology (NIST). Prior to joining NIST, he was on the engineering faculty (1986-1994) at the Massachusetts Institute of Technology (MIT) and was instrumental in setting up the Intelligent Engineering Systems Laboratory. Sriram has co-authored or authored more than 275 publications, and is a Fellow of ASME, AAAS, IEEE and Washington Academy of Sciences, a Distinguished Member (life) of ACM and a Senior Member (life) of AAAI.

Peak Wavelength Inflection Law

Thomas S. Kakovitch¹, Russell R. Vane III², David Lambert Jr.²

¹University of the District of Columbia ²Fusion Energy Partners, LLC

Abstract

In this paper we use Planck's Blackbody Radiation Law, which governs the intensity of radiation emitted per unit surface area at a fixed temperature, to discover its second derivative to find inflection points. This radiation has a computable although small energy.

Introduction

A BLACK BODY ACTS AS A MEDIUM that has its own optical density in which radiation (even though being part of the electromagnetic spectrum) becomes trapped for a long time. A blackbody eventually comes into equilibrium with its surroundings. Its distribution of energy in terms of both wavelength and frequency follows Planck's function. When the slopes of Planck's function are zero, an effective peak wavelength or an effective peak frequency occurs. These peaks are not solely functions of wavelength and frequency *but also temperature* (different stars produce different effective peaks because of their temperature).

By computing the second derivative of Planck's Function in terms of wavelength and temperature, and setting it to zero, we will derive a point of inflection.

Method

The spectral emissive power per unit area, per unit solid angle, per unit wavelength of wavelength λ for fixed temperature θ is given by the Planck's Blackbody Radiation function:

$$B(\lambda, \theta) = \frac{2hc^2}{(-1 + e^{\frac{hc}{k\theta\lambda}})\lambda^5} \quad (1)$$

The first derivative (with respect to λ) of which is:

$$\frac{\partial B(\lambda, \theta)}{\partial \lambda} = \frac{2h^2c^3e^{\frac{hc}{k\theta\lambda}}}{(-1 + e^{\frac{hc}{k\theta\lambda}})^2k\theta\lambda^7} - \frac{10hc^2}{(-1 + e^{\frac{hc}{k\theta\lambda}})\lambda^6} \quad (2)$$

Setting Equation (2) to zero and solving for λ obtains (Kakovitch et al., 2022):

$$\lambda_{peak} = \frac{hc}{k\theta(5 + W_0(-5e^{-5}))} \quad (3)$$

where W_0 is the principal branch of the Lambert W function. The fact that the peak wavelength is inversely proportional to temperature is called Wien's displacement law.

The second derivative of Equation (1) with respect to λ is:

$$\frac{\partial^2 B(\lambda, \theta)}{\partial \lambda^2} = \frac{4c^4 e^{\frac{2hc}{k\theta\lambda}} h^3}{(-1 + e^{\frac{hc}{k\theta\lambda}})^3 k^2 \theta^2 \lambda^9} - \frac{2c^4 e^{\frac{hc}{k\theta\lambda}} h^3}{(-1 + e^{\frac{hc}{k\theta\lambda}})^2 k^2 \theta^2 \lambda^9} - \frac{24c^3 e^{\frac{hc}{k\theta\lambda}} h^2}{(-1 + e^{\frac{hc}{k\theta\lambda}})^2 k\theta\lambda^8} + \frac{60c^2 h}{(-1 + e^{\frac{hc}{k\theta\lambda}})\lambda^7} \quad (4)$$

We used the symbolic and computational power of Mathematica® to obtain the results in this article. Subsequent equations have been copied verbatim from a Mathematica session.

A request to Mathematica to set Equation (4) to zero and solve produced the following two solutions:

$$\lambda_1 = \frac{\frac{1}{60} \left(\frac{c h}{1 + e^{\frac{c h}{k \theta \lambda}}} \right)^2 k^2 \theta^2 \left(12 c e^{\frac{c h}{k \theta \lambda}} \left(-1 + e^{\frac{c h}{k \theta \lambda}} \right) h k \theta - \sqrt{144 c^2 e^{\frac{2 c h}{k \theta \lambda}} \left(-1 + e^{\frac{c h}{k \theta \lambda}} \right)^2 h^2 k^2 \theta^2 - 120 \left(-1 + e^{\frac{c h}{k \theta \lambda}} \right)^2 \left(2 c^2 e^{\frac{c h}{k \theta \lambda}} h^2 + c^2 e^{\frac{c h}{k \theta \lambda}} \left(-1 + e^{\frac{c h}{k \theta \lambda}} \right) h^2 \right) k^2 \theta^2} \right)}{h^2 k^2 \theta^2} \quad (5)$$

$$\lambda_2 = \frac{\frac{1}{60} \left(\frac{c h}{-1 + e^{\frac{c h}{k \theta \lambda}}} \right)^2 k^2 \theta^2 \left(12 c e^{\frac{c h}{k \theta \lambda}} \left(-1 - e^{\frac{c h}{k \theta \lambda}} \right) h k \theta + \sqrt{144 c^2 e^{\frac{2 c h}{k \theta \lambda}} \left(1 + e^{\frac{c h}{k \theta \lambda}} \right)^2 h^2 k^2 \theta^2 - 120 \left(1 + e^{\frac{c h}{k \theta \lambda}} \right)^2 \left(2 c^2 e^{\frac{c h}{k \theta \lambda}} h^2 + c^2 e^{\frac{c h}{k \theta \lambda}} \left(-1 + e^{\frac{c h}{k \theta \lambda}} \right) h^2 \right) k^2 \theta^2} \right)}{h^2 k^2 \theta^2} \quad (6)$$

We include the actual formulation in this paper in the Appendix so that they may be verified in Equations (7) through (10). Mathematica's graphics were used to show in the subsequent figures where the inflection points of Planck's Blackbody Radiation Law occur.

The Sun is approximately a blackbody with temperature approximately equal to 5790 K. For this temperature the output of Equations (5) and (6) are exactly the same.

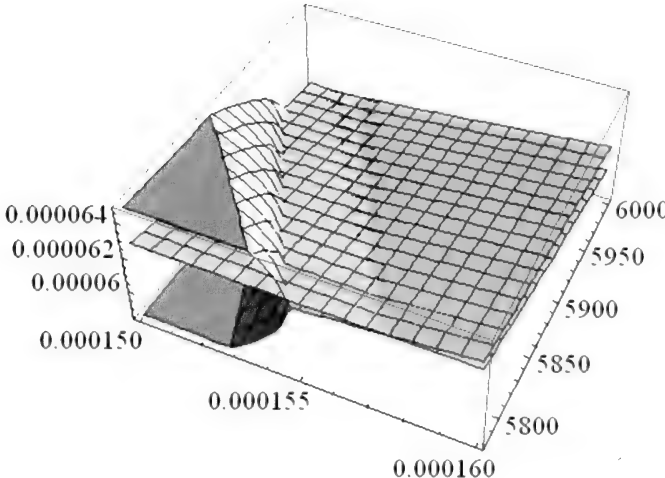


Figure 1: A 3-D plot of Equations (5), (6), (7) and (8).

To scale Equations (3), (7), and (8) onto the same graph, we set the constants below to obtain the approximate values of Equations (5) and (6):

$$C1 = 1.25$$

$$C2 = 0.44860025265327175$$

The 3-D plot of Equations (3), (5), and (6) times $C1$, and (7) and (8) times $C2$ in the range of $0.00015 \leq \lambda \leq 0.00016$ and $5780 \leq \theta \leq 6000$ is shown in Figure 1. We observe the near vicinity around $\lambda = 0.000155$ cm for a possible anomaly.

In the Appendix we have computed the mass, m_j in Equation (9). A variety of 3-D plots of m_j are shown in Figures 2, 3 and 4.

Finding

Stars radiating at temperatures from 5780 to 6000 K, such as our Sun, show anomalies of approximately 2 ev and slightly higher. These anomalies appear in the yellow range of the electromagnetic spectrum.

We are unable to determine if this effect is due to a resonance or a composite particle of other constituents. It is significantly smaller than an electron.

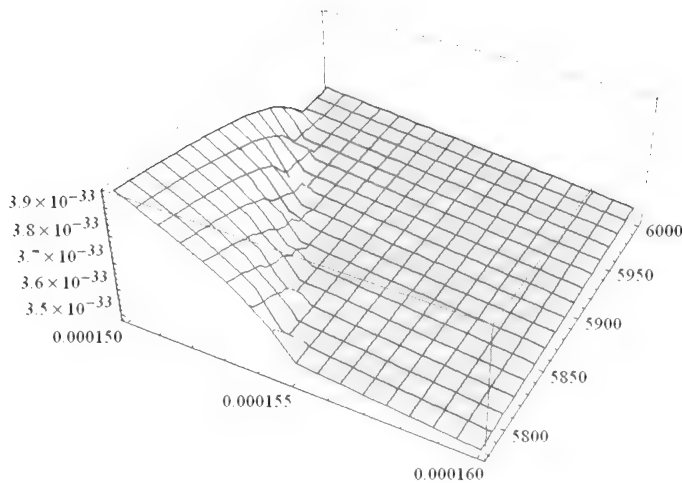


Figure 2: The 3-D plot of Equation (9) gives the magnitude of m_j in grams for λ near 0.000155 cm.

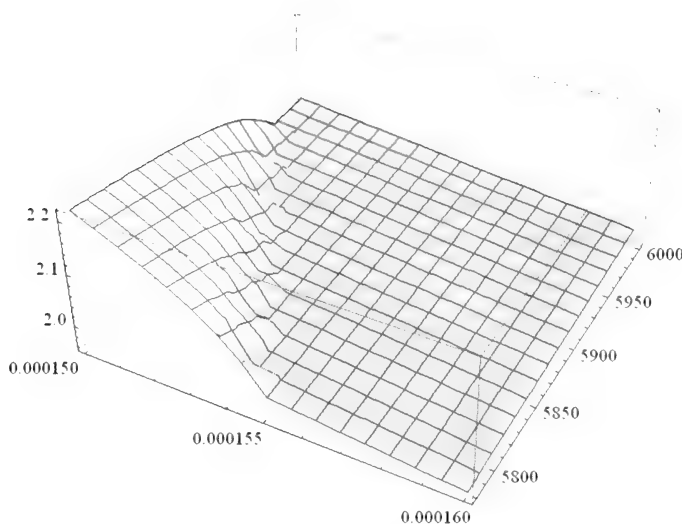


Figure 3: The 3-D plot of Equation (9) in magnitude of electron volts (eV) for λ near 0.000155 cm.

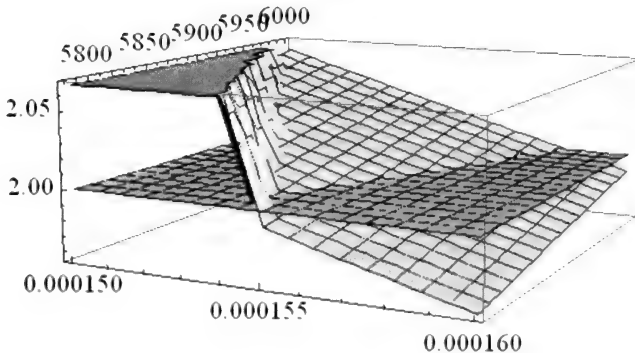


Figure 4: A 3-D plot of Equation (9) with a 2 eV plane superimposed for reference.

Conclusion

The blackbody shows an optical density that has an index of refraction which is the inverse of the constant from Equation (10) from Kakovitch et al. (2022) as follows:

$$\lambda_{peak} \nu_{peak} = \frac{3 + W_0(-3e^{-3})}{5 + W_0(-5e^{-5})} c \approx 0.5682526605497431311c, \quad (7)$$

where W_0 is the principal branch of the Lambert W function. This inverse is ≈ 1.898 . By comparison, water has an index of refraction of 1.3325. Blackbody radiation behaves as a substance with its own specific index of refraction of approximately 1.898.

Glossary

$c = 299792458 \text{ m/s}$ is the speed of light in a vacuum (exact).

$e = 2.71828182845904523536\dots$ is Euler's number.

$h = 6.62607015 \times 10^{-34} \text{ J}\cdot\text{Hz}^{-1}$ is Planck's constant (exact).

$k = 1.380649 \times 10^{-23} \text{ J}\cdot\text{K}^{-1}$ is the Boltzmann constant (exact).

Appendix

This is a Mathematica® version of the calculations discussed. Equating Equation (3) to Equation (5) and solving for λ in terms of θ obtains a real solution (7):

$$\lambda 1\alpha = \frac{(c h) \sqrt{\left(k \theta \operatorname{Log}\left(\left(25+22 \operatorname{ProductLog}\left[-\frac{5}{e^5}\right]-\operatorname{ProductLog}\left[-\frac{5}{e^5}\right]^2\right.\right.\right.}}{\left.\left.\left.\sqrt{1225+1340 \operatorname{ProductLog}\left[-\frac{5}{e^5}\right]+414 \operatorname{ProductLog}\left[-\frac{5}{e^5}\right]^2+44 \operatorname{ProductLog}\left[-\frac{5}{e^5}\right]^3+\operatorname{ProductLog}\left[-\frac{5}{e^5}\right]^4}\right)\right)\right.} \left(2\left(-5-2 \operatorname{ProductLog}\left[-\frac{5}{e^5}\right]+\operatorname{ProductLog}\left[-\frac{5}{e^5}\right]^2\right)\right) \quad (8)$$

The Mathematica notation for $W_0(z)$ is $\operatorname{ProductLog}[z]$, and the notation for $W_k(z)$ is $\operatorname{ProductLog}[k, z]$. Equating Equation (3) to Equation (6) and solving for λ in terms of θ obtains an imaginary solution (8):

$$\lambda 2\alpha = \frac{(c h) \sqrt{\left(k \theta \left(i \pi+\operatorname{Log}\left(\left(25+22 \operatorname{ProductLog}\left[-\frac{5}{e^5}\right]+\operatorname{ProductLog}\left[-\frac{5}{e^5}\right]^2\right.\right.\right.\right.\right.\right.}}{\left.\left.\left.\left.\left.\left.\sqrt{1225+1340 \operatorname{ProductLog}\left[-\frac{5}{e^5}\right]+414 \operatorname{ProductLog}\left[-\frac{5}{e^5}\right]^2+44 \operatorname{ProductLog}\left[-\frac{5}{e^5}\right]^3+\operatorname{ProductLog}\left[-\frac{5}{e^5}\right]^4}\right)\right)\right)\right)\right)\right.} \left(2\left(-5-2 \operatorname{ProductLog}\left[-\frac{5}{e^5}\right]+\operatorname{ProductLog}\left[-\frac{5}{e^5}\right]^2\right)\right) \quad (9)$$

Setting the Compton wavelength of Equation (5) and solving for the respective anomaly in terms of mass, m_j , as per Equation (9):

$$\text{Solve}[\text{Norm}[\lambda 1]==h/(m j*c), m j] \quad (10)$$

we obtain Equation (10):

$$m_j = \frac{\left(2.20999 \times 10^{37}\right) \operatorname{Norm}\left[1 / \left(\left(-1+e^{\frac{225230727}{156545701 \theta^2}}\right)^2 \theta^2\right)\right]}{874608471337363316186760085504 \left(\frac{e^{\frac{225230727}{156545701 \theta^2}} \left(1+e^{\frac{225230727}{156545701 \theta^2}}\right) \theta}{3039465308968388588492906443393}\right)} \\ m_j = \frac{\frac{198811881}{66311230 \lambda} \left(-1-e^{\frac{225230727}{156545701 \lambda}}\right)^2 \theta^2}{9238349364422302047098425625312288442505195673270064009707520} \\ m_j = \left| -1+e^{\frac{225230727}{156545701 \theta^2}} \right|^2 \left(\frac{\frac{225230727}{156545701 \theta^2}}{1267548802612526367093/207425341} + \frac{e^{\frac{225230727}{156545701 \theta^2}} \left(1+e^{\frac{225230727}{156545701 \theta^2}}\right)}{25350816052250527741874414853682} \right) \theta^2 \right\} \quad (11)$$

References

Burden, Richard L. and Faires, J. Douglas (1985), “2.1 The Bisection Algorithm,” *Numerical Analysis* (3rd ed.), PWS Publishers, ISBN 0-87150-857-5

Joos, Georg (1986) *Theoretical Physics*, (Mineola NY: Dover), pp. 621-624

Kakovitch, Thomas S. (2012) *The Fifth Force*, (Amherst MA: HDR Press), p.19

Kakovitch, T. S., Vane, R.R., Lambert, D.R. (2022) “Frequency Displacement Law,” *Journal of the Washington Academy of Sciences* Volume 108 Number 1 Spring 2022, p. 45-48

Weidner, Richard T. & Sells, Robert L., (1960) *Elementary Modern Physics*, (Boston, MA: Allyn & Bacon), p. 455

PROFESSOR THOMAS S. KAKOVITCH is a professor emeritus at University of District of Columbia. He holds 26 US Patents. He has written five books, including the seminal, *The Fifth Force*, published in 2012.

RUSSELL VANE, PhD, investigates discrepancies in the standard physics models for FEP. He served until 2021 as a futurist in the National Risk Management Center.

DAVID LAMBERT JR. was the Principal Investigator for Service Oriented Architectures for Northrop Gumman Information Technologies. He serves Fusion Energy Partners as its Chemistry Lead.

The Shape of Planck's Law

Kenneth Baclawski
Northeastern University

Abstract

Planck's Law describes the spectral density of electromagnetic radiation emitted by a black body at a temperature T . While it is well known that the "shape" of Planck's Law is independent of the temperature, it is not clear what is meant by the shape of a function. In this note, a notion of shape is introduced and Planck's Law is shown to have the same shape for every temperature. This property of a family of functions can be useful for computing properties of the functions.

Introduction

PLANCK'S LAW is a function that describes an important property of entities in thermal equilibrium. In this note, we introduce a simple notion of "shape" and show that Planck's Law has the same shape for any temperature. Planck's Law at a particular temperature is actually several functions, depending on the spectral variable, such as frequency, wavelength, wavenumber and the angular versions of these three. Each of these forms of Planck's Law is a family of functions, and the functions within one family have the same shape. We illustrate the shape of the forms of Planck's Law for frequency and wavelength.

The notion of the shape of a function can be useful for computing properties of families of functions, all of which have the same shape. We illustrate this by showing some properties of the forms of Planck's Law for frequency and wavelength.

The Shape of a Function

In geometry, two subsets of a Euclidean space have the *same shape* if one can be transformed to the other by a combination of translations, rotations (together also called rigid transformations), and uniform scalings (Kendall, 1984). Sometimes mirror images are also considered to have the same shape. While the graph of a function is a geometrical figure, this definition of shape is not entirely satisfactory, because the domain and range should be preserved by the transformation. Accordingly, we define two functions f and g to have the same shape if there is a

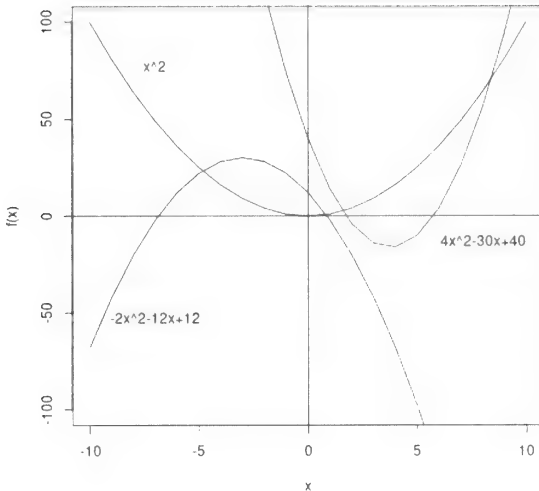


Figure 1: Some examples of quadratic functions

nonsingular affine transformation that bijectively maps the graph of f onto the graph of g , and that the affine transformation is the direct product of transformations on the domain and range, each of which is a combination of rigid transformations, uniform scalings and/or reflections. For the case of real-valued functions of a single variable, $f(x)$ and $g(x)$, this means that there are constants $p \neq 0$, q , $r \neq 0$, and s , such that for every x , $f(x) = pg(rx + s) + q$, and for every y , $g(y) = \frac{1}{p}f(\frac{y-s}{r}) - \frac{q}{p}$.

To understand the notion of the shape of a function, we first consider a simpler case: quadratic functions. If one plots some examples of quadratic functions as in Figure 1, it seems clear that all quadratic functions have the same shape. In general, if $f(x)$ be the quadratic function $ax^2 + bx + c$, where $a \neq 0$, Then one can transform $f(x)$ to x^2 by using $p = a$, $q = \frac{4ac-b^2}{4a}$, $r = 1$, and $s = \frac{b}{2a}$. In other words, one can “normalize” every quadratic function to the “standard” quadratic function x^2 . Thus every quadratic function has the same shape. For example, the quadratic function given by $f(x) = -2x^2 - 12x + 12$ in Figure 1, can be transformed to x^2 by $f(x) = -2(x + 3)^2 + 30$.

The special case where the transformation does not include a

translation is especially useful because the zeroes of the function and all of its derivatives transform in the same way as the function. More precisely, if $f(x) = pg(rx)$, then x_0 is a zero of f if and only if x_0/r is a zero of g . Since $f'(x) = prg'(rx)$, it follows that x_1 is a zero of f' if and only if x_1/r is a zero of g' , and similarly for higher derivatives. In particular, the maxima, minima and inflection points of f all transform to maxima, minima and inflection points of g by the same transformation.

Planck's Laws

Planck's Law with respect to the frequency of electromagnetic radiation is the spectral emissive power per unit area, per unit solid angle, per unit frequency. The formula is

$$B_\nu(\nu, T) = \frac{2h\nu^3}{c^2} \left(e^{\frac{h\nu}{kT}} - 1 \right)^{-1} \quad (1)$$

where ν is the frequency in Hz, T is the absolute temperature in kelvins, h is Planck's constant, c is the speed of light in a vacuum, and k is the Boltzmann constant. The SI units of B_ν are $W \cdot sr^{-1} \cdot m^{-2} \cdot Hz^{-1}$.

Another form of Planck's Law uses wavelength rather than frequency. The formula is

$$B_\lambda(\lambda, T) = \frac{2hc^2}{\lambda^5} \left(e^{\frac{hc}{kT\lambda}} - 1 \right)^{-1} \quad (2)$$

where λ is the wavelength. This form is not the same as simply expressing $B_\nu(\nu, T)$ in terms of λ . The electromagnetic radiation is measured as the spectral emissive power per unit area, per unit solid angle, per unit wavelength. The SI units of B_λ are $W \cdot sr^{-1} \cdot m^{-3}$.

The Shape of Planck's Law

We now show that each of the forms of Planck's Law in Equations (1) and (2) have the property that all functions in each family have the same shape. Looking at Equation (1), it is not easy to see how one might transform the functions for different temperatures into each other. The way to do this is to "normalize" the frequency and spectral density to obtain a function that does not depend on the temperature T , as we did

for quadratic functions.¹ In fact, it should be easier because we now have just one parameter T , while the family of quadratic functions has three parameters, a , b and c . First consider the family of functions $B_\nu(\nu, T)$ defined in Equation (1). We want to find $p \neq 0$ and $r \neq 0$ such that the function $pB_\nu(rx, T)$ does not depend on T . Note that both q and s must be 0 because the domain and range of B_ν are the positive real numbers. The parameter T only occurs once in $B_\nu(\nu, T)$, and setting $r = T$ will cancel that occurrence of T as follows:

$$B_\nu(Tx, T) = \frac{2h(Tx)^3}{c^2} \left(e^{\frac{h(Tx)}{kT}} - 1 \right)^{-1} = \frac{2hT^3x^3}{c^2} \left(e^{\frac{hx}{k}} - 1 \right)^{-1} \quad (3)$$

This eliminated the parameter T in the exponent, but now T occurs in another location. However, this is easily eliminated by setting $p = T^{-3}$ to get

$$T^{-3}B_\nu(Tx, T) = T^{-3} \frac{2hT^3x^3}{c^2} \left(e^{\frac{hx}{k}} - 1 \right)^{-1} = \frac{2hx^3}{c^2} \left(e^{\frac{hx}{k}} - 1 \right)^{-1} \quad (4)$$

This solves the problem of showing that the family of Planck's Law functions with respect to the frequency all have the same shape. It also proves that the maximum of any member of this family occurs at a frequency that is proportional to T . A similar process shows that the family of functions $B_\lambda(\lambda, T)$ have the same shape and that the maximum value occurs at a wavelength that is proportional to T^{-1} . The latter fact is known as Wien's Displacement Law.

A better normalization of B_ν would be to simplify the function as much as possible as follows:

$$\frac{h^2c^2}{2k^3T^3} B_\nu \left(\frac{kT}{h}x, T \right) = \frac{h^2c^2}{2k^3T^3} \frac{2h}{c^2} \left(\frac{kT}{h}x \right)^3 (e^x - 1)^{-1} = \frac{x^3}{e^x - 1} \quad (5)$$

The normalized function in Equation (5) is shown in Figure 2, along with the first and second derivatives.

Similarly, one can simplify B_λ as much as possible as follows:

$$\frac{h^4c^3}{2k^5T^5} B_\lambda \left(\frac{hc}{kT}x, T \right) = \frac{h^4c^3}{2k^5T^5} \frac{2hc^2}{\left(\frac{hc}{kT}x \right)^5} (e^{1/x} - 1)^{-1} = \frac{1}{(e^{1/x} - 1)x^5} \quad (6)$$

¹Such a normalized function need not necessarily be a Planck's Law function for any temperature, but it is mathematically a function with the same shape.

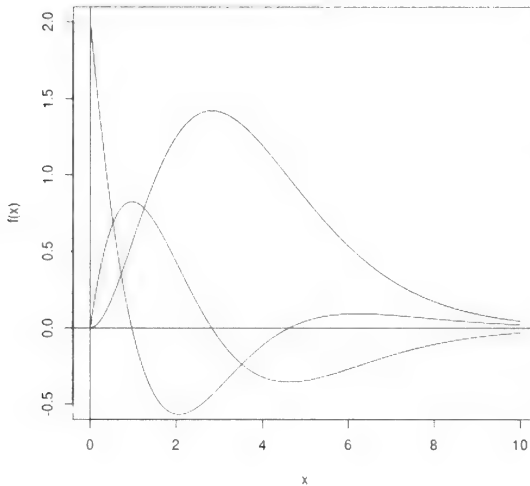


Figure 2: The normalized Planck's Law with respect to frequency and its first and second derivatives.

The normalized function in Equation (6) is shown in Figure 3 along with its first and second derivatives. Unlike the case of the normalization of B_ν , one cannot easily show the normalization of B_λ along with its derivatives in a single graph because the scales of the function and its derivatives are very different.

The advantage of the normalized functions for Planck's Laws is that properties of the normalized functions will apply to all the Planck's Laws. For example, one can find the peak frequency and peak wavelength as well as the inflection points by using a bisection algorithm (Burden and Faires, 1985). The two inflection points of the frequency form of Planck's law are approximately

$$0.3424733308258767159414181 \nu_{peak}$$

$$1.6386129484772208568940635 \nu_{peak}$$

and the two inflection points of the wavelength form of Planck's law are approximately

$$0.5879674557934156285307749 \lambda_{peak}$$

$$1.4088873906179916088985216 \lambda_{peak}.$$

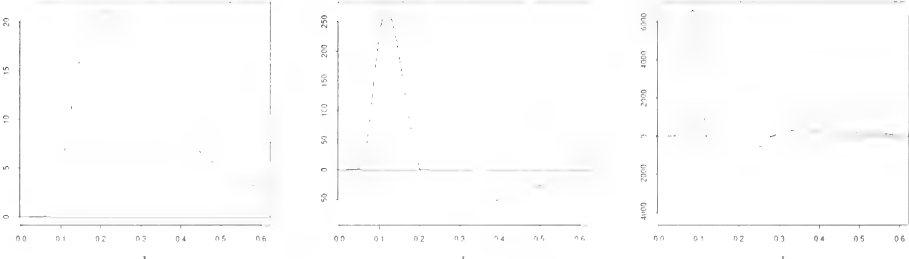


Figure 3: The normalized Planck's Law with respect to wavelength and its first and second derivatives.

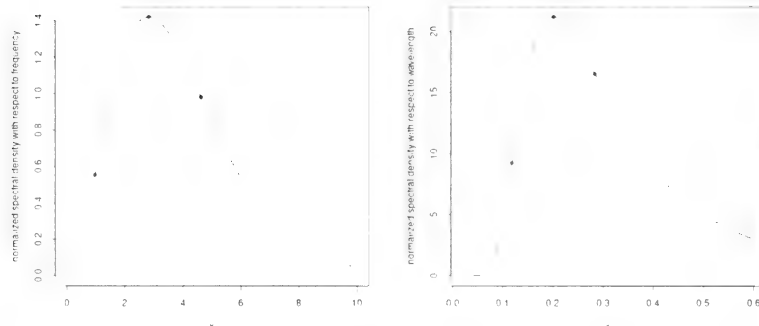


Figure 4: The normalized Planck's Laws with respect to wavelength and frequency with the peaks and inflection points indicated with dots.

The peaks and inflection points are shown using dots on Figure 4. The Sun is approximately a black body with a temperature of about 5790 K. For this temperature, the peak wavelength is $\lambda_{peak} \approx 500$ nm, and the inflection points have wavelengths that are approximately 295 nm and 706 nm.

All of the most commonly used forms of Planck's Law have the same shape as either Equation (5) or Equation (6). The wave number form of Planck's Law has the same shape as the frequency form of Planck's Law, and the angular forms of Planck's Law have the same shape as the corresponding ordinary forms.

Glossary

$c = 299792458$ m/s is the speed of light in a vacuum (exact).

$e = 2.71828182845904523536\dots$ is Euler's number.

$h = 6.62607015 \times 10^{-34}$ J·Hz $^{-1}$ is Planck's constant (exact).

$k = 1.380649 \times 10^{-23}$ J·K $^{-1}$ is the Boltzmann constant (exact).

References

Burden, Richard L. and Faires, J. Douglas (1985), "2.1 The Bisection Algorithm," *Numerical Analysis* (3rd ed.), PWS Publishers, ISBN 0-87150-857-5

Kendall, D.G. (1984). "Shape Manifolds, Procrustean Metrics, and Complex Projective Spaces," in Bulletin of the London Mathematical Society. 16(2): 81–121. doi:10.1112/blms/16.2.81.

KENNETH BACLAWSKI is an Associate Professor Emeritus at the College of Computer and Information Science, Northeastern University. Professor Baclawski does research in data semantics, formal methods for software engineering and software modeling, data mining in biology and medicine, semantic collaboration tools, situation awareness, information fusion, self-aware and self-adaptive systems, and wireless communication. He is a member of the Washington Academy of Sciences, IEEE, ACM, IAOA, and is the chair of the Board of Trustees of the Ontolog Forum.

Delegates to the Washington Academy of Sciences Representing Affiliated Scientific Societies

Acoustical Society of America	Paul Arveson
American/International Association of Dental Research	J. Terrell Hoffeld
American Association of Physics Teachers, Chesapeake Section	Frank R. Haig, S. J.
American Astronomical Society	Sethanne Howard
American Fisheries Society	Lee Benaka
American Institute of Aeronautics and Astronautics	David W. Brandt
American Institute of Mining, Metallurgy & Exploration	E. Lee Bray
American Meteorological Society	Vacant
American Nuclear Society	Charles Martin
American Phytopathological Society	Vacant
American Society for Cybernetics	Stuart Umpleby
American Society for Microbiology	Vacant
American Society of Civil Engineers	Vacant
American Society of Mechanical Engineers	Daniel J. Vavrick
American Society of Plant Physiology	Mark Holland
Anthropological Society of Washington	Vacant
ASM International	Toni Marechaux
Association for Women in Science	Jodi Wesemann
Association for Computing Machinery	Vacant
Association for Science, Technology, and Innovation	F. Douglas Witherspoon
Association of Information Technology Professionals	Vacant
Biological Society of Washington	Vacant
Botanical Society of Washington	Chris Puttock
Capital Area Food Protection Association	Keith Lempel
Chemical Society of Washington	Vacant
District of Columbia Institute of Chemists	Vacant
Eastern Sociological Society	Ronald W. Mandersheid
Electrochemical Society	Vacant
Entomological Society of Washington	Vacant
Geological Society of Washington	Jeff Plescia Jurate Landwehr
Historical Society of Washington DC	Vacant
Human Factors and Ergonomics Society	Gerald Krueger

(continued on next page)

Delegates to the Washington Academy of Sciences Representing Affiliated Scientific Societies

(continued from previous page)

Institute of Electrical and Electronics Engineers, Washington Section	Richard Hill
Institute of Food Technologies, Washington DC Section	Taylor Wallace
Institute of Industrial Engineers, National Capital Chapter	Neal F. Schmeidler
International Association for Dental Research, American Section	Christopher Fox
International Society for the Systems Sciences	Vacant
International Society of Automation, Baltimore Washington Section	Richard Sommerfield
Instrument Society of America	Hank Hegner
Marine Technology Society	Jake Sobin
Maryland Native Plant Society	Vacant
Mathematical Association of America, Maryland-District of Columbia-Virginia Section	John Hamman
Medical Society of the District of Columbia	Julian Craig
National Capital Area Skeptics	Vacant
National Capital Astronomers	Jay H. Miller
National Geographic Society	Vacant
Optical Society of America, National Capital Section	Jim Heaney
Pest Science Society of America	Vacant
Philosophical Society of Washington	Michael P. Cohen
Society for Experimental Biology and Medicine	Vacant
Society of American Foresters, National Capital Society	Marilyn Buford
Society of American Military Engineers, Washington DC Post	Vacant
Society of Manufacturing Engineers, Washington DC Chapter	Vacant
Society of Mining, Metallurgy, and Exploration, Inc., Washington DC Section	E. Lee Bray
Soil and Water Conservation Society, National Capital Chapter	Erika Larsen
Technology Transfer Society, Washington Area Chapter	Richard Leshuk
Virginia Native Plant Society, Potomac Chapter	Alan Ford
Washington DC Chapter of the Institute for Operations Research and the Management Sciences (WINFORMS)	Meagan Pitluck-Schmitt
Washington Evolutionary Systems Society	Vacant
Washington History of Science Club	Albert G. Gluckman
Washington Paint Technology Group	Vacant
Washington Society of Engineers	Alvin Reiner
Washington Society for the History of Medicine	Alain Touwaide
Washington Statistical Society	Michael P. Cohen
World Future Society, National Capital Region Chapter	Jim Honig

Washington Academy of Sciences
Room 455
1200 New York Ave. NW
Washington, DC 20005
Return Postage Guaranteed

NONPROFIT ORG
US POSTAGE PAID
MERRIFIELD VA 22081
PERMIT# 888



4*7*****98*****AUTO**MIXED ADC 207

HARVARD LAW S LIB ERSMCZ

LANGDELL HALL 152

1545 MASSACHUSETTS AVE

CAMBRIDGE, MA 02138-2903